92 Kobayashi D, Zeller M, Cole T *et al.* *BACE1* gene deletion: impact on behavioral function in a model of Alzheimer's disease. *Neurobiol. Aging* 29(6), 861–873 (2008).

93 Dominguez D, Tournoy J, Hartmann D *et al.* Phenotypic and biochemical analyses of BACE1- and BACE2-deficient mice. *J. Biol. Chem.* 280(35), 30797–30806 (2005).

94 Hu X, Hicks CW, He W *et al.* Bace1 modulates myelination in the central and peripheral nervous system. *Nat. Neurosci.* 9(12), 1520–1525 (2006).

95 Willem M, Garratt AN, Novak B *et al.* Control of peripheral nerve myelination by the β-secretase BACE1. *Science* 314(5799), 664–666 (2006).

96 Hu X, He W, Diaconu C *et al.* Genetic deletion of BACE1 in mice affects remyelination of sciatic nerves. *FASEB J.* 22(8), 2970–2980 (2008).

97 Savonenko AV, Melnikova T, Laird FM *et al.* Alteration of BACE1-dependent NRG1/ErbB4 signaling and schizophrenia-like phenotypes in BACE1-null mice. *Proc. Natl Acad. Sci. USA* 105(14), 5585–5590 (2008).

98 Dejaegere T, Serneels L, Schafer MK *et al.* Deficiency of Aph1B/C-γ-secretase disturbs Nrg1 cleavage and sensorimotor gating that can be reversed with antipsychotic treatment. *Proc. Natl Acad. Sci. USA* 105(28), 9775–9780 (2008).

99 Sankaranarayanan S, Price EA, Wu G *et al.* *In vivo* β-secretase 1 inhibition leads to brain Aβ lowering and increased α-secretase processing of amyloid precursor protein without effect on neuregulin-1. *J. Pharmacol. Exp. Ther.* 324(3), 957–969 (2008).

100 McConlogue L, Buttini M, Anderson JP *et al.* Partial reduction of BACE1 has dramatic effects on Alzheimer plaque and synaptic pathology in APP transgenic Mice. *J. Biol. Chem.* 282(36), 26326–26334 (2007).

101 Levitan D, Greenwald I. Facilitation of lin-12-mediated signalling by sel-12, a *Caenorhabditis elegans* S182 Alzheimer's disease gene. *Nature* 377(6547), 351–354 (1995).

102 Struhl G, Greenwald I. Presenilin is required for activity and nuclear access of Notch in *Drosophila*. *Nature* 398(6727), 522–525 (1999).

103 Ye Y, Lukinova N, Fortini ME. Neurogenic phenotypes and altered Notch processing in *Drosophila* presenilin mutants. *Nature* 398(6727), 525–529 (1999).

104 Doerfler P, Shearman MS, Perlmutter RM. Presenilin-dependent γ-secretase activity modulates thymocyte development. *Proc. Natl Acad. Sci. USA* 98(16), 9312–9317 (2001).

105 Hadland BK, Manley NR, Su D *et al.* γ-secretase inhibitors repress thymocyte development. *Proc. Natl Acad. Sci. USA* 98(13), 7487–7491 (2001).

106 Geling A, Steiner H, Willem M, Bally-Cuif L, Haass C. A γ-secretase inhibitor blocks Notch signaling *in vivo* and causes a severe neurogenic phenotype in zebrafish. *EMBO Rep.* 3(7), 688–694 (2002).

107 Cheng HT, Miner JH, Lin M *et al.* γ-secretase activity is dispensable for mesenchyme-to-epithelium transition but required for podocyte and proximal tubule formation in developing mouse kidney. *Development* 130(20), 5031–5042 (2003).

108 Micchelli CA, Esler WP, Kimberly WT *et al.* γ-secretase/presenilin inhibitors for Alzheimer's disease phenocopy Notch mutations in *Drosophila*. *FASEB J.* 17(1), 79–81 (2003).

109 Searfoss GH, Jordan WH, Calligaro DO *et al.* Adipsin, a biomarker of gastrointestinal toxicity mediated by a functional γ-secretase inhibitor. *J. Biol. Chem.* 278(46), 46107–46116 (2003).

110 Milano J, McKay J, Dagenais C *et al.* Modulation of notch processing by γ-secretase inhibitors causes intestinal goblet cell metaplasia and induction of genes known to specify gut secretory lineage differentiation. *Toxicol. Sci.* 82(1), 341–358 (2004).

111 Wong GT, Manfra D, Poulet FM *et al.* Chronic treatment with the γ-secretase inhibitor LY-411,575 inhibits β-amyloid peptide production and alters lymphopoiesis and intestinal cell differentiation. *J. Biol. Chem.* 279(13), 12876–12882 (2004).

112 Kopan R, Schroeter EH, Weintraub H, Nye JS. Signal transduction by activated mNotch: importance of proteolytic processing and its regulation by the extracellular domain. *Proc. Natl Acad. Sci. USA* 93(4), 1683–1688 (1996).

113 Talora C, Campese AF, Bellavia D *et al.* Notch signaling and diseases: an evolutionary journey from a simple beginning to complex outcomes. *Biochim. Biophys. Acta* 1782(9), 489–497 (2008).

114 Lathia JD, Mattson MP, Cheng A. Notch: from neural development to neurological disorders. *J. Neurochem.* 107(6), 1471–1481 (2008).

115 Gordon WR, Arnett KL, Blacklow SC. The molecular logic of Notch signalling – a structural and biochemical perspective. *J. Cell Sci.* 121(Pt 19), 3109–3119 (2008).

116 Ilagan MX, Kopan R. SnapShot: notch signaling pathway. *Cell* 128(6), 1246 (2007).

117 Parks AL, Curtis D. Presenilin diversifies its portfolio. *Trends Genet.* 23(3), 140–150 (2007).

118 Beel AJ, Sanders CR. Substrate specificity of γ-secretase and other intramembrane proteases. *Cell. Mol. Life Sci.* 65(9), 1311–1334 (2008).

119 Qian S, Jiang P, Guan XM *et al.* Mutant human presenilin 1 protects presenilin 1 null mouse against embryonic lethality and elevates Aβ1–42/43 expression. *Neuron* 20(3), 611–617 (1998).

120 Yu H, Saura CA, Choi SY *et al.* APP processing and synaptic plasticity in presenilin-1 conditional knockout mice. *Neuron* 31(5), 713–726 (2001).

121 Saura CA, Choi SY, Beglopoulos V *et al.* Loss of presenilin function causes impairments of memory and synaptic plasticity followed by age-dependent neurodegeneration. *Neuron* 42(1), 23–36 (2004).

122 Choi SH, Veeraraghavalu K, Lazarov O *et al.* Non-cell-autonomous effects of presenilin 1 variants on enrichment-mediated hippocampal progenitor cell proliferation and differentiation. *Neuron* 59(4), 568–580 (2008).

123 Niidome T, Taniuchi N, Akaike A, Kihara T, Sugimoto H. Differential regulation of neurogenesis in two neurogenic regions of APPswe/PS1dE9 transgenic mice. *Neuroreport* 19(14), 1361–1364 (2008).

124 Rodriguez JJ, Jones VC, Tabuchi M *et al.* Impaired adult neurogenesis in the dentate gyrus of a triple transgenic mouse model of Alzheimer's disease. *PLoS ONE* 3(8), e2935 (2008).

125 De Strooper B. Loss-of-function presenilin mutations in Alzheimer disease. Talking point on the role of presenilin mutations in Alzheimer disease. *EMBO Rep.* 8(2), 141–146 (2007).

126 Wolfe MS. When loss is gain: reduced presenilin proteolytic function leads to increased Aβ42/Aβ40. Talking point on the role of presenilin mutations in Alzheimer disease. *EMBO Rep.* 8(2), 136–140 (2007).

127 Shen J, Kelleher RJ 3rd. The presenilin hypothesis of Alzheimer's disease: evidence for a loss-of-function pathogenic mechanism. *Proc. Natl Acad. Sci. USA* 104(2), 403–409 (2007).

128 Hong L, Koelsch G, Lin X *et al.* Structure of the protease domain of memapsin 2 (β-secretase) complexed with inhibitor. *Science* 290(5489), 150–153 (2000).

129 Shimizu H, Tosaki A, Kaneko K *et al.* Crystal structure of an active form of BACE1, an enzyme responsible for amyloid β protein production. *Mol. Cell Biol.* 28(11), 3663–3671 (2008).

130 Nguyen JT, Hamada Y, Kimura T, Kiso Y. Design of potent aspartic protease inhibitors to treat various diseases. *Arch. Pharm. (Weinheim)* 341(9), 523–535 (2008).

131 Ghosh AK, Kumaragurubaran N, Hong L *et al.* Potent memapsin 2 (β-secretase) inhibitors: design, synthesis, protein-ligand x-ray structure, and *in vivo* evaluation. *Bioorg. Med. Chem. Lett.* 18(3), 1031–1036 (2008).

132 Hamada Y, Ohta H, Miyamoto N *et al.* Novel non-peptidic and small-sized BACE1 inhibitors. *Bioorg. Med. Chem. Lett.* 18(5), 1643–1647 (2008).

133 Hussain I, Hawkins J, Harrison D *et al.* Oral administration of a potent and selective non-peptidic BACE-1 inhibitor decreases β-cleavage of amyloid precursor protein and amyloid-β production *in vivo*. *J. Neurochem.* 100(3), 802–809 (2007).

134 Cole DC, Stock JR, Chopra R et al. Acylguanidine inhibitors of β-secretase: optimization of the pyrrole ring substituents extending into the S1 and S3 substrate binding pockets. *Bioorg. Med. Chem. Lett.* 18(3), 1063–1066 (2008).

135 Baxter EW, Conway KA, Kennis L *et al.* 2-amino-3,4-dihydroquinazolines as inhibitors of BACE-1 (β-site APP cleaving enzyme): use of structure based design to convert a micromolar hit into a nanomolar lead. *J. Med. Chem.* 50(18), 4261–4264 (2007).

136 van Es JH, van Gijn ME, Riccio O *et al.* Notch/γ-secretase inhibition turns proliferative cells in intestinal crypts and adenomas into goblet cells. *Nature* 435(7044), 959–963 (2005).

137 Fleisher AS, Raman R, Siemers ER *et al.* Phase II safety trial targeting amyloid β production with a γ-secretase inhibitor in Alzheimer disease. *Arch. Neurol.* 65(8), 1031–1038 (2008).

138 Siemers ER, Dean RA, Friedrich S *et al.* Safety, tolerability, and effects on plasma and cerebrospinal fluid amyloid-β after inhibition of γ-secretase. *Clin. Neuropharmacol.* 30(6), 317–325 (2007).

139 Siemers ER, Quinn JF, Kaye J *et al.* Effects of a γ-secretase inhibitor in a randomized study of patients with Alzheimer disease. *Neurology* 66(4), 602–604 (2006).

140 Siemers E, Skinner M, Dean RA *et al.* Safety, tolerability, and changes in amyloid β concentrations after administration of a γ-secretase inhibitor in volunteers. *Clin. Neuropharmacol.* 28(3), 126–132 (2005).

141 in t'Veld BA, Ruitenberg A, Hofman A *et al.* Nonsteroidal antiinflammatory drugs and the risk of Alzheimer's disease. *N. Engl. J. Med.* 345(21), 1515–1521 (2001).

142 Aisen PS, Schafer KA, Grundman M *et al.* Effects of rofecoxib or naproxen vs placebo on Alzheimer disease progression: a randomized controlled trial. *JAMA* 289(21), 2819–2826 (2003).

143 Martin BK, Szekely C, Brandt J *et al.* Cognitive function over time in the Alzheimer's Disease Anti-inflammatory Prevention Trial (ADAPT): results of a randomized, controlled trial of naproxen and celecoxib. *Arch. Neurol.* 65(7), 896–905 (2008).

144 Weggen S, Eriksen JL, Das P *et al.* A subset of NSAIDs lower amyloidogenic Aβ42 independently of cyclooxygenase activity. *Nature* 414(6860), 212–216 (2001).

145 Morihara T, Chu T, Ubeda O, Beech W, Cole GM. Selective inhibition of Aβ42 production by NSAID R-enantiomers. *J. Neurochem.* 83(4), 1009–1012 (2002).

146 Eriksen JL, Sagi SA, Smith TE *et al.* NSAIDs and enantiomers of flurbiprofen target γ-secretase and lower Aβ42 *in vivo*. *J. Clin. Invest.* 112(3), 440–449 (2003).

147 Takahashi Y, Hayashi I, Tominari Y *et al.* Sulindac sulfide is a noncompetitive γ-secretase inhibitor that preferentially reduces Aβ42 generation. *J. Biol. Chem.* 278(20), 18664–18670 (2003).

148 Beher D, Clarke EE, Wrigley JD *et al.* Selected non-steroidal anti-inflammatory drugs and their derivatives target γ-secretase at a novel site. Evidence for an allosteric mechanism. *J. Biol. Chem.* 279(42), 43419–43426 (2004).

149 Kukar T, Murphy MP, Eriksen JL *et al.* Diverse compounds mimic Alzheimer disease-causing mutations by augmenting Aβ42 production. *Nat. Med.* 11(5), 545–550 (2005).

150 Czech C, Burns MP, Vardanian L *et al.* Cholesterol independent effect of LXR agonist TO-901317 on γ-secretase. *J. Neurochem.* 101(4), 929–936 (2007).

151 Kukar TL, Ladd TB, Bann MA *et al.* Substrate-targeting γ-secretase modulators. *Nature* 453(7197), 925–929 (2008).

152 Narlawar R, Baumann K, Czech C, Schmidt B. Conversion of the LXR-agonist TO-901317 – from inverse to normal modulation of γ-secretase by addition of a carboxylic acid and a lipophilic anchor. *Bioorg. Med. Chem. Lett.* 17(19), 5428–5431 (2007).

153 Kukar T, Prescott S, Eriksen JL *et al.* Chronic administration of R-flurbiprofen attenuates learning impairments in transgenic amyloid precursor protein mice. *BMC Neurosci.* 8, 54 (2007).

154 Imbimbo BP, Del Giudice E, Colavito D *et al.* 1-(3',4'-Dichloro-2-fluoro.1,1'-biphenyl]-4-yl)-cyclopropanecarboxylic acid (CHF5074), a novel γ-secretase modulator, reduces brain β-amyloid pathology in a transgenic mouse model of Alzheimer's disease without causing peripheral toxicity. *J. Pharmacol. Exp. Ther.* 323(3), 822–830 (2007).

155 Page RM, Baumann K, Tomioka M *et al.* Generation of Aβ38 and Aβ42 is independently and differentially affected by familial Alzheimer disease-associated presenilin mutations and γ-secretase modulation. *J. Biol. Chem.* 283(2), 677–683 (2008).

156 Barten DM, Guss VL, Corsa JA *et al.* Dynamics of β-amyloid reductions in brain, cerebrospinal fluid, and plasma of β-amyloid precursor protein transgenic mice treated with a γ-secretase inhibitor. *J. Pharmacol. Exp. Ther.* 312(2), 635–643 (2005).

157 Tian G, Sobotka-Briner CD, Zysk J *et al.* Linear non-competitive inhibition of solubilized human γ-secretase by pepstatin A methylester, L685458, sulfonamides, and benzodiazepines. *J. Biol. Chem.* 277(35), 31499–31505 (2002).

158 Tian G, Ghanekar SV, Aharony D *et al.* The mechanism of γ-secretase: multiple inhibitor binding sites for transition state analogs and small molecule inhibitors. *J. Biol. Chem.* 278(31), 28968–28975 (2003).

159 Clarke EE, Churcher I, Ellis S *et al.* Intra- or intercomplex binding to the γ-secretase enzyme. A model to differentiate inhibitor classes. *J. Biol. Chem.* 281(42), 31279–31289 (2006).

160 Kreft A, Harrison B, Aschmies S *et al.* Discovery of a novel series of Notch-sparing γ-secretase inhibitors. *Bioorg. Med. Chem. Lett.* 18(14), 4232–4236 (2008).

161 Mayer SC, Kreft AF, Harrison B *et al.* Discovery of begacestat, a Notch-1-sparing γ-secretase inhibitor for the treatment of Alzheimer's disease. *J. Med. Chem.* 51(23), 7348–7351 (2008).

162 Arbel M, Yacoby I, Solomon B. Inhibition of amyloid precursor protein processing by β-secretase through site-directed antibodies. *Proc. Natl Acad. Sci. USA* 102(21), 7718–7723 (2005).

163 Paganetti P, Calanca V, Galli C, Stefani M, Molinari M. β-site specific intrabodies to decrease and prevent generation of Alzheimer's Aβ peptide. *J. Cell Biol.* 168(6), 863–868 (2005).

164 Chang WP, Downs D, Huang XP *et al.* Amyloid-β reduction by memapsin 2 (β-secretase) immunization. *FASEB J.* 21(12), 3184–3196 (2007).

165 O'Connor T, Sadleir KR, Maus E *et al.* Phosphorylation of the translation initiation factor eIF2α increases BACE1 levels and promotes amyloidogenesis. *Neuron* 60(6), 988–1009 (2008).

166 Faghihi MA, Modarresi F, Khalil AM *et al.* Expression of a noncoding RNA is elevated in Alzheimer's disease and drives rapid feed-forward regulation of β-secretase. *Nat. Med.* 14(7), 723–730 (2008).

167 Wang WX, Rajeev BW, Stromberg AJ *et al.* The expression of microRNA miR-107 decreases early in Alzheimer's disease and may accelerate disease progression through regulation of β-site amyloid precursor protein-cleaving enzyme 1. *J. Neurosci.* 28(5), 1213–1223 (2008).

168 Hebert SS, Horre K, Nicolai L *et al.* Loss of microRNA cluster miR-29a/b-1 in sporadic Alzheimer's disease correlates with increased BACE1/β-secretase expression. *Proc. Natl Acad. Sci. USA* 105(17), 6415–6420 (2008).

169 Boissonneault V, Plante I, Rivest S, Provost P. MicroRNA-298 and microRNA-328 regulate expression of mouse β-amyloid precursor protein-converting enzyme 1. *J. Biol. Chem.* 284(4), 1971–1981 (2009).

170 Ratovitski T, Slunt HH, Thinakaran G *et al.* Endoproteolytic processing and stabilization of wild-type and mutant presenilin. *J. Biol. Chem.* 272(39), 24536–24541 (1997).

171 Zhang J, Kang DE, Xia W *et al.* Subcellular distribution and turnover of presenilins in transfected cells. *J. Biol. Chem.* 273(20), 12436–12442 (1998).

172 Thinakaran G, Harris CL, Ratovitski T *et al.* Evidence that levels of presenilins (PS1 and PS2) are coordinately regulated by competition for limiting cellular factors. *J. Biol. Chem.* 272(45), 28415–28422 (1997).

173 Donoviel DB, Hadjantonakis AK, Ikeda M *et al.* Mice lacking both presenilin genes exhibit early embryonic patterning defects. *Genes Dev.* 13(21), 2801–2810 (1999).

174 Lai MT, Chen E, Crouthamel MC *et al.* Presenilin-1 and presenilin-2 exhibit distinct yet overlapping γ-secretase activities. *J. Biol. Chem.* 278(25), 22475–22481 (2003).

175 Cheng H, Vetrivel KS, Gong P *et al.* Mechanisms of disease: new therapeutic strategies for Alzheimer's disease – targeting APP processing in lipid rafts. *Nat. Clin. Pract. Neurol.* 3(7), 374–382 (2007).

176 Thinakaran G, Koo EH. Amyloid precursor protein trafficking, processing, and function. *J. Biol. Chem.* 283(44), 29615–29619 (2008).

177 Tesco G, Koh YH, Kang EL *et al.* Depletion of GGA3 stabilizes BACE and enhances β-secretase activity. *Neuron* 54(5), 721–737 (2007).

178 Sisodia SS, St George-Hyslop PH. γ-secretase, Notch, Aβ and Alzheimer's disease: where do the presenilins fit in? *Nat. Rev. Neurosci.* 3(4), 281–290 (2002).

179 Kaether C, Lammich S, Edbauer D *et al.* Presenilin-1 affects trafficking and processing of βAPP and is targeted in a complex with nicastrin to the plasma membrane. *J. Cell Biol.* 158(3), 551–561 (2002).

180 Spasic D, Annaert W. Building γ-secretase: the bits and pieces. *J. Cell Sci.* 121(Pt 4), 413–420 (2008).

181 Fukumori A, Okochi M, Tagami S *et al.* Presenilin-dependent γ-secretase on plasma membrane and endosomes is functionally distinct. *Biochemistry* 45(15), 4907–4914 (2006).

182 Thathiah A, Spittaels K, Hoffmann M *et al.* The orphan G protein-coupled receptor 3 modulates amyloid-β peptide generation in neurons. *Science* 323(5916), 946–951 (2009).

183 Ehehalt R, Keller P, Haass C, Thiele C, Simons K. Amyloidogenic processing of the Alzheimer β-amyloid precursor protein depends on lipid rafts. *J. Cell Biol.* 160(1), 113–123 (2003).

184 Simons K, Toomre D. Lipid rafts and signal transduction. *Nat. Rev. Mol. Cell Biol.* 1(1), 31–39 (2000).

185 Helms JB, Zurzolo C. Lipids as targeting signals: lipid rafts and intracellular trafficking. *Traffic* 5(4), 247–254 (2004).

186 Sakurai T, Kaneko K, Okuno M *et al.* Membrane microdomain switching: a regulatory mechanism of amyloid precursor protein processing. *J. Cell Biol.* 183(2), 339–352 (2008).

187 Postina R, Schroeder A, Dewachter I *et al.* A disintegrin-metalloproteinase prevents amyloid plaque formation and hippocampal defects in an Alzheimer disease mouse model. *J. Clin. Invest.* 113(10), 1456–1464 (2004).

188 Marcade M, Bourdin J, Loiseau N *et al.* Etazolate, a neuroprotective drug linking GABA(A) receptor pharmacology to amyloid precursor protein processing. *J. Neurochem.* 106(1), 392–404 (2008).

189 Sastre M, Steiner H, Fuchs K *et al.* Presenilin-dependent γ-secretase processing of β-amyloid precursor protein at a site corresponding to the S3 cleavage of Notch. *EMBO Rep.* 2(9), 835–841 (2001).

190 Gu Y, Misonou H, Sato T *et al.* Distinct intramembrane cleavage of the β-amyloid precursor protein family resembling γ-secretase-like cleavage of Notch. *J. Biol. Chem.* 276(38), 35235–35238 (2001).

191 Yu C, Kim SH, Ikeuchi T *et al.* Characterization of a presenilin-mediated amyloid precursor protein carboxyl-terminal fragment γ. Evidence for distinct mechanisms involved in γ-secretase processing of the APP and Notch1 transmembrane domains. *J. Biol. Chem.* 276(47), 43756–43760 (2001).

192 Kimberly WT, Zheng JB, Guenette SY, Selkoe DJ. The intracellular domain of the β-amyloid precursor protein is stabilized by Fe65 and translocates to the nucleus in a notch-like manner. *J. Biol. Chem.* 276(43), 40288–40292 (2001).

193 Okochi M, Steiner H, Fukumori A *et al.* Presenilins mediate a dual intramembranous γ-secretase cleavage of Notch-1. *EMBO J.* 21(20), 5408–5416 (2002).

194 Zhao G, Cui MZ, Mao G *et al.* γ-cleavage is dependent on ζ-cleavage during the proteolytic processing of amyloid precursor protein within its transmembrane domain. *J. Biol. Chem.* 280(45), 37689–37697 (2005).

195 Qi-Takahara Y, Morishima-Kawashima M, Tanimura Y *et al.* Longer forms of amyloid β protein: implications for the mechanism of intramembrane cleavage by γ-secretase. *J. Neurosci.* 25(2), 436–445 (2005).

196 Sato T, Nyborg AC, Iwata N *et al.* Signal peptide peptidase: biochemical properties and modulation by nonsteroidal antiinflammatory drugs. *Biochemistry* 45(28), 8649–8656 (2006).

197 Fluhrer R, Grammer G, Israel L *et al.* A γ-secretase-like intramembrane cleavage of TNFα by the GxGD aspartyl protease SPPL2b. *Nat. Cell Biol.* 8(8), 894–896 (2006).

198 Fluhrer R, Fukumori A, Martin L *et al.* Intramembrane proteolysis of GXGD-type aspartyl proteases is slowed by a familial Alzheimer disease-like mutation. *J. Biol. Chem.* 283(44), 30121–30128 (2008).

199 Sato T, Ananda K, Cheng CI *et al.* Distinct pharmacological effects of inhibitors of signal peptide peptidase and γ-secretase. *J. Biol. Chem.* 283(48), 33287–33295 (2008).

200 Hemming ML, Elias JE, Gygi SP, Selkoe DJ. Proteomic profiling of γ-secretase substrates and mapping of substrate requirements. *PLoS Biol.* 6(10), e257 (2008).

201 Lemberg MK, Martoglio B. Requirements for signal peptide peptidase-catalyzed intramembrane proteolysis. *Mol. Cell* 10(4), 735–744 (2002).

202 Martin L, Fluhrer R, Haass C. Substrate Requirements for SPPL2b-dependent regulated intramembrane proteolysis. *J. Biol. Chem.* 284(9), 5662–5670 (2009).

203 Munter LM, Voigt P, Harmeier A *et al.* GxxxG motifs within the amyloid precursor protein transmembrane sequence are critical for the etiology of Aβ42. *EMBO J.* 26(6), 1702–1712 (2007).

204 Kienlen-Campard P, Tasiaux B, Van Hees J *et al.* Amyloidogenic processing but not amyloid precursor protein (APP) intracellular C-terminal domain production requires a precisely oriented APP dimer assembled by transmembrane GXXXG motifs. *J. Biol. Chem.* 283(12), 7733–7744 (2008).

205 Sato T, Tang TC, Reubins G *et al.* A helix-to-coil transition at the epsilon-cut site in the transmembrane dimer of the amyloid precursor protein is required for proteolysis. *Proc. Natl Acad. Sci. USA* 106(5), 1421–1426 (2009).

206 Urban S, Freeman M. Substrate specificity of rhomboid intramembrane proteases is governed by helix-breaking residues in the substrate transmembrane domain. *Mol. Cell* 11(6), 1425–1434 (2003).

207 Ye J, Dave UP, Grishin NV, Goldstein JL, Brown MS. Asparagine-proline sequence within membrane-spanning segment of SREBP triggers intramembrane cleavage by site-2 protease. *Proc. Natl Acad. Sci. USA* 97(10), 5123–5128 (2000).

208 Urban S, Wolfe MS. Reconstitution of intramembrane proteolysis *in vitro* reveals that pure rhomboid is sufficient for catalysis and specificity. *Proc. Natl Acad. Sci. USA* 102(6), 1883–1888 (2005).

209 Tomita T, Chang TY, Kodama T, Iwatsubo T. βAPP γ-secretase and SREBP site 2 protease are two different enzymes. *Neuroreport* 9(5), 911–913 (1998).

210 Annaert WG, Esselens C, Baert V *et al.* Interaction with telencephalin and the amyloid precursor protein predicts a ring structure for presenilins. *Neuron* 32(4), 579–589 (2001).

211 Tomita T, Takikawa R, Koyama A *et al.* C terminus of presenilin is required for overproduction of amyloidogenic Aβ42 through stabilization and endoproteolysis of presenilin. *J. Neurosci.* 19(24), 10627–10634 (1999).

212 Kaether C, Capell A, Edbauer D *et al.* The presenilin C-terminus is required for ER-retention, nicastrin-binding and γ-secretase activity. *EMBO J.* 23(24), 4738–4748 (2004).

213 Bergman A, Laudon H, Winblad B, Lundkvist J, Naslund J. The extreme C terminus of presenilin 1 is essential for γ-secretase complex assembly and activity. *J. Biol. Chem.* 279(44), 45564–45572 (2004).

214 Futai E, Yagishita S, Ishiura S. Nicastrin is dispensable for γ-secretase protease activity in the presence of specific presenilin mutations. *J. Biol. Chem.* DOI: 10.1074/jbc.M807653200 (2009) (Epub ahead of print).

215 Das C, Berezovska O, Diehl TS *et al.* Designed helical peptides inhibit an intramembrane protease. *J. Am. Chem. Soc.* 125(39), 11794–11795 (2003).

216 Kornilova AY, Bihel F, Das C, Wolfe MS. The initial substrate-binding site of γ-secretase is located on presenilin near the active site. *Proc. Natl Acad. Sci. USA* 102(9), 3230–3235 (2005).

217 Morohashi Y, Kan T, Tominari Y *et al.* C-terminal fragment of presenilin is the molecular target of a dipeptidic γ-secretase-specific inhibitor DAPT (N-.N-(3,5-difluorophenacetyl)-L-alanyl]-S-phenylglycine t-butyl ester). *J. Biol. Chem.* 281(21), 14670–14676 (2006).

218 Fuwa H, Takahashi Y, Konno Y *et al.* Divergent synthesis of multifunctional molecular probes to elucidate the enzyme specificity of dipeptidic γ-secretase inhibitors. *ACS Chem. Biol.* 2(6), 408–418 (2007).

219 Kornilova AY, Das C, Wolfe MS. Differential effects of inhibitors on the γ-secretase complex. Mechanistic implications. *J. Biol. Chem.* 278(19), 16470–16473 (2003).

220 Weihofen A, Lemberg MK, Friedmann E *et al.* Targeting presenilin-type aspartic protease signal peptide peptidase with γ-secretase inhibitors. *J. Biol. Chem.* 278(19), 16528–16533 (2003).

221 Nyborg AC, Jansen K, Ladd TB, Fauq A, Golde TE. A signal peptide peptidase (SPP) reporter activity assay based on the cleavage of type II membrane protein substrates provides further evidence for an inverted orientation of the SPP active site relative to presenilin. *J. Biol. Chem.* 279(41), 43148–43156 (2004).

222 Lemberg MK, Bland FA, Weihofen A, Braud VM, Martoglio B. Intramembrane proteolysis of signal peptides: an essential step in the generation of HLA-E epitopes. *J. Immunol.* 167(11), 6441–6446 (2001).

223 McLauchlan J, Lemberg MK, Hope G, Martoglio B. Intramembrane proteolysis promotes trafficking of hepatitis C virus core protein to lipid droplets. *EMBO J.* 21(15), 3980–3988 (2002).

224 Nyborg AC, Ladd TB, Jansen K, Kukar T, Golde TE. Intramembrane proteolytic cleavage by human signal peptide peptidase like 3 and malaria signal peptide peptidase. *FASEB J.* 20(10), 1671–1679 (2006).

225 Friedmann E, Hauben E, Maylandt K *et al.* SPPL2a and SPPL2b promote intramembrane proteolysis of TNFα in activated dendritic cells to trigger IL-12 production. *Nat. Cell Biol.* 8(8), 843–848 (2006).

226 Grigorenko AP, Moliaka YK, Soto MC, Mello CC, Rogaev EI. The *Caenorhabditis elegans IMPAS* gene, imp-2, is essential for development and is functionally distinct from related presenilins. *Proc. Natl Acad. Sci. USA* 101(41), 14955–14960 (2004).

227 Casso DJ, Tanda S, Biehs B, Martoglio B, Kornberg TB. *Drosophila* signal peptide peptidase is an essential protease for larval development. *Genetics* 170(1), 139–148 (2005).

228 Zhao B, Yu M, Neitzel M *et al.* Identification of γ-secretase inhibitor potency determinants on presenilin. *J. Biol. Chem.* 283(5), 2927–2938 (2008).

229 Fuwa H, Hiromoto K, Takahashi Y *et al.* Synthesis of biotinylated photoaffinity probes based on arylsulfonamide γ-secretase inhibitors. *Bioorg. Med. Chem. Lett.* 16(16), 4184–4189 (2006).

230 Hung LW, Ciccotosto GD, Giannakis E *et al.* Amyloid-β peptide (Aβ) neurotoxicity is modulated by the rate of peptide aggregation: Aβ dimers and trimers correlate with neurotoxicity. *J. Neurosci.* 28(46), 11950–11958 (2008).

231 Espeseth AS, Xu M, Huang Q *et al.* Compounds that bind APP and inhibit Aβ processing *in vitro* suggest a novel approach to Alzheimer disease therapeutics. *J. Biol. Chem.* 280(18), 17792–17797 (2005).

232 Lleo A, Berezovska O, Herl L *et al.* Nonsteroidal anti-inflammatory drugs lower Aβ42 and change presenilin 1 conformation. *Nat. Med.* 10(10), 1065–1066 (2004).

233 Karlin A, Akabas MH. Substituted-cysteine accessibility method. *Methods Enzymol.* 293, 123–145 (1998).

234 Seal RP, Leighton BH, Amara SG. Transmembrane topology mapping using biotin-containing sulfhydryl reagents. *Methods Enzymol.* 296, 318–331 (1998).

235 Sato C, Morohashi Y, Tomita T, Iwatsubo T. Structure of the catalytic pore of γ-secretase probed by the accessibility of substituted cysteines. *J. Neurosci.* 26(46), 12081–12088 (2006).

236 Tolia A, Chavez-Gutierrez L, De Strooper B. Contribution of presenilin transmembrane domains 6 and 7 to a water-containing cavity in the γ-secretase complex. *J. Biol. Chem.* 281(37), 27633–27642 (2006).

237 Sato C, Takagi S, Tomita T, Iwatsubo T. The C-terminal PAL motif and transmembrane domain 9 of presenilin 1 are involved in the formation of the catalytic pore of the γ-secretase. *J. Neurosci.* 28(24), 6264–6271 (2008).

238 Tolia A, Horre K, De Strooper B. Transmembrane domain 9 of presenilin determines the dynamic conformation of the catalytic site of γ-secretase. *J. Biol. Chem.* 283(28), 19793–19803 (2008).

239 Lazarov VK, Fraering PC, Ye W *et al.* Electron microscopic structure of purified, active γ-secretase reveals an aqueous intramembrane chamber and two pores. *Proc. Natl Acad. Sci. USA* 103(18), 6889–6894 (2006).

240 Osenkowski P, Li H, Ye W *et al.* Cryoelectron microscopy structure of purified γ-secretase at 12 A resolution. *J. Mol. Biol.* 385(2), 642–652 (2009).

241 Urban S, Shi Y. Core principles of intramembrane proteolysis: comparison of rhomboid and site-2 family proteases. *Curr. Opin. Struct. Biol.* 18(4), 432–441 (2008).

242 Koch U, Radtke F. Notch and cancer: a double-edged sword. *Cell. Mol. Life Sci.* 64(21), 2746–2762 (2007).

243 Rizzo P, Osipo C, Foreman K *et al.* Rational targeting of Notch signaling in cancer. *Oncogene* 27(38), 5124–5131 (2008).

244 Yan M, Plowman GD. Delta-like 4/Notch signaling and its therapeutic implications. *Clin. Cancer Res.* 13(24), 7243–7246 (2007).

245 Ischenko I, Seeliger H, Schaffer M, Jauch KW, Bruns CJ. Cancer stem cells: how can we target them? *Curr. Med. Chem.* 15(30), 3171–3184 (2008).

246 Wang Z, Li Y, Banerjee S, Sarkar FH. Emerging role of Notch in stem cells and cancer. *Cancer Lett.* DOI: 10.1016/j.canlet.2008.09.030 (2008) (Epub ahead of print).

247 Real PJ, Tosello V, Palomero T *et al.* γ-secretase inhibitors reverse glucocorticoid resistance in T cell acute lymphoblastic leukemia. *Nat. Med.* 15(1), 50–58 (2009).

248 Reiss K, Saftig P. The 'a disintegrin and metalloprotease' (ADAM) family of sheddases: physiological and cellular functions. *Semin. Cell Dev. Biol.* 20(2), 126–137 (2009).

249 Parsons RB, Austen BM. Protein–protein interactions in the assembly and subcellular trafficking of the BACE (β-site amyloid precursor protein-cleaving enzyme) complex of Alzheimer's disease. *Biochem. Soc. Trans.* 35(Pt 5), 974–979 (2007).


### *Patents*


301 PERSEUS PROTEOMICS INC.: WO2007129457 (2007)

302 VLAAMS INTERUNIVERSITAIR INSTITUUT VOOR BIOTECHNOLOGIE VZW: WO2004026331 (2004)


### *Website*


401 Alzheimer disease & frontotemporal dementia mutation database www.molgen.ua.ac.be/ADMutations


### Affiliation


• Taisuke Tomita
Department of Neuropathology and Neuroscience, Graduate School of Pharmaceutical Sciences, The University of Tokyo, Bunkyo, Tokyo 113–0033, Japan
Tel.: +81 358 414 868
Fax: +81 358 414 708
taisuke@mol.f.u-tokyo.ac.jp

J|A|C|S
ARTICLES

Published on Web 05/11/2009

# Inhibition of γ-Secretase Activity by Helical β-Peptide Foldamers

Yuki Imamura,[†] Naoto Watanabe,[‡] Naoki Umezawa,*[,†] Takeshi Iwatsubo,[‡,¶,§] Nobuki Kato,[†] Taisuke Tomita,*[,‡,¶] and Tsunehiko Higuchi*[,†]

*Graduate School of Pharmaceutical Sciences, Nagoya City University, 3-1 Tanabe-dori, Mizuho-ku, Nagoya, Aichi 467-8603, and Graduate School of Pharmaceutical Sciences, Core Research for Evolutional Science and Technology (CREST), Japan Science and Technology Corporation, and Graduate School of Medicine, The University of Tokyo, 7-3-1 Hongo, Bunkyo-ku, Tokyo 113-0033*

Received January 8, 2009; E-mail: umezawa@phar.nagoya-cu.ac.jp; taisuke@mol.f.u-tokyo.ac.jp; higuchi@phar.nagoya-cu.ac.jp

***Abstract:*** Alzheimer's disease (AD) is a neurodegenerative disorder pathologically characterized by extensive extracellular deposition of amyloid-β (Aβ) peptides as senile plaques, and inhibition of "amyloidogenic" amyloid precursor protein (APP) processing by γ-secretase is an important strategy for prevention and treatment of AD. Here we show that β-peptide foldamers designed to adopt a 12-helical conformation in solution are potent and specific inhibitors of γ-secretase. Subtle modifications that disrupt helicity substantially reduce inhibitory potency, suggesting that helical conformation is critical for effective inhibition. These β-peptides competed with helical peptide-type inhibitor, suggesting that they interact with the substrate binding site of γ-secretase. The β-peptide with inhibitory activity at nanomolar concentration should be a useful lead compound for development of γ-secretase-specific inhibitors and molecular tools to explore substrate recognition by intramembrane proteases.

## Introduction

Alzheimer's disease (AD) is a neurodegenerative disorder that is characterized by extracellular deposition of amyloid-β (Aβ) peptides as senile plaques.[1,2] γ-Secretase, a membrane-embedded aspartic protease comprising presenilin (PS), nicastrin, Aph-1 and Pen-2, is responsible for the proteolytic processing of amyloid precursor protein (APP) within the transmembrane domain to generate Aβ peptides. Thus, inhibition or modulation of γ-secretase activity is a potentially effective strategy for the treatment of AD.[3,4] A number of γ-secretase inhibitors (GSIs) have been identified, including peptidic transition-state analogues (TSAs) that directly block the active site.[3,4] α-Aminoisobutyric acid (Aib)-based helical peptides designed to mimic the APP transmembrane domain also inhibit γ-secretase activity by targeting the initial substrate docking site.[5,6] We hypothesized that unnatural oligomers with well-defined conformations ("foldamers")[7−9] can mimic the helical APP transmembrane domain and thereby inhibit γ-secretase activity. Here, we describe the development of oligomers of β-amino acids ("β-peptides") that interact with the substrate docking site of γ-secretase. β-Peptides are attractive unnatural scaffolds, because they adopt predictable helical conformations[8,10] and resist proteolysis.[11,12] Also, their oligomeric nature makes combinatorial design straightforward.

## Results and Discussion

**Foldamer Design and Secondary Structure Analysis.** We designed simple oligomers of conformationally restricted β-amino acids, β-peptides **1**−**6** (Figure 1). Enantiomers of trans-2-aminocyclopentanecarboxylic acid (ACPC) were chosen as the building blocks since their oligomers are fairly hydrophobic; γ-secretase cleaves hydrophobic membrane protein. Also, the oligomers of enantiomerically pure ACPC form stable 12-helix structure (defined by 12-membered ring C=O($i$) → H−N($i$+3) hydrogen bonds), which could be a good mimic of the α-helix in terms of overall shape.[8,10,13] CD spectra of **1**−**6** in methanol are presented in Figure 2. β-Peptides **1**−**3** display a shallow minimum at ~222 nm and a maximum at 204−205 nm, which

[†] Nagoya City University.
[‡] Graduate School of Pharmaceutical Sciences, The University of Tokyo.
[¶] CREST.
[§] Graduate School of Medicine, The University of Tokyo.

(1) Selkoe, D. J. *J. Clin. Invest.* **2002**, *110*, 1375–1381.
(2) Wolfe, M. S. *Nat. Rev. Drug Discov.* **2002**, *1*, 859–866.
(3) Tomita, T.; Iwatsubo, T. *Curr. Pharm. Des.* **2006**, *12*, 661–670.
(4) Wolfe, M. S. *Neurotherapeutics* **2008**, *5*, 391–398.
(5) Das, C.; Berezovska, O.; Diehl, T. S.; Genet, C.; Buldyrev, I.; Tsai, J. Y.; Hyman, B. T.; Wolfe, M. S. *J. Am. Chem. Soc.* **2003**, *125*, 11794–11795.
(6) Kornilova, A. Y.; Bihel, F.; Das, C.; Wolfe, M. S. *Proc. Natl. Acad. Sci. U.S.A.* **2005**, *102*, 3230–3235.
(7) Gellman, S. H. *Acc. Chem. Res.* **1998**, *31*, 173–180.
(8) Cheng, R. P.; Gellman, S. H.; DeGrado, W. F. *Chem. Rev.* **2001**, *101*, 3219–3232.
(9) Hill, D. J.; Mio, M. J.; Prince, R. B.; Hughes, T. S.; Moore, J. S. *Chem. Rev.* **2001**, *101*, 3893–4012.
(10) Lee, H.-S.; Syud, F. A.; Wang, X.; Gellman, S. H. *J. Am. Chem. Soc.* **2001**, *123*, 7721–7722.
(11) Frackenpohl, J.; Arvidsson, P. I.; Schreiber, J. V.; Seebach, D. *ChemBioChem* **2001**, *2*, 445–55.
(12) Porter, E. A.; Weisblum, B.; Gellman, S. H. *J. Am. Chem. Soc.* **2002**, *124*, 7324–7330.
(13) Appella, D. H.; Christianson, L. A.; Klein, D. A.; Powell, D. R.; Huang, X.; Barchi, J. J., Jr.; Gellman, S. H. *Nature* **1997**, *387*, 381–384.

10.1021/ja9001458 CCC: $40.75 

| Peptides | Sequence | Number of β-amino acids |
|---|---|---|
| 1 | Ac-$X^R X^R X^R X^R X^R X^R$-$NH_2$ | 6 |
| 2 | Ac-$X^R X^R X^R X^R X^R X^R X^R X^R X^R$-$NH_2$ | 9 |
| 3 | Ac-$X^R X^R X^R X^R X^R X^R X^R X^R X^R X^R X^R X^R$-$NH_2$ | 12 |
| 4 | Ac-$X^S X^S X^S X^S X^S X^S$-$NH_2$ | 6 |
| 5 | Ac-$X^S X^S X^S X^S X^S X^S X^S X^S X^S$-$NH_2$ | 9 |
| 6 | Ac-$X^S X^S X^S X^S X^S X^S X^S X^S X^S X^S X^S X^S$-$NH_2$ | 12 |

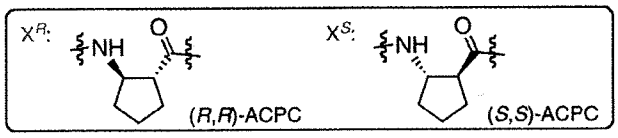


***Figure 1.*** Synthesized helical β-peptide foldamers.

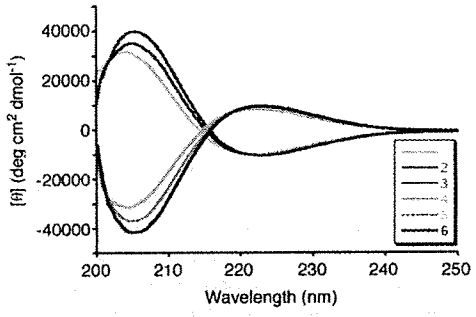


***Figure 2.*** CD spectra of β-peptides **1-6** in methanol. The molar ellipticity [θ] values have been normalized for oligomer concentration and the number of backbone amide groups.

***Table 1.*** Inhibitory Potency of β-Peptides **1**−**6** toward γ-Secretase

| compound | $IC_{50}$ (Aβ40, nM) | $IC_{50}$ (Aβ42, nM) |
|---|---|---|
| **1** | $>3.00 \times 10^4$ | $>3.00 \times 10^4$ |
| **2** | $2.87 \times 10^3$ | $>3.00 \times 10^4$ |
| **3** | $9.78 \times 10^2$ | $1.23 \times 10^4$ |
| **4** | $>3.00 \times 10^4$ | $>3.00 \times 10^4$ |
| **5** | 19.8 | $3.77 \times 10^3$ |
| **6** | 5.24 | 6.93 |

are characteristic of left-handed 12-helical β-peptides.[13−15] The increase in intensity at 222 nm with additional ACPC residues indicates that the population of the 12-helical state increases as the β-peptide length increases. β-Peptides **4-6** had mirror-image CD spectra compared with their enantiomers **1**−**3**, within experimental error.

**γ-Secretase Inhibitory Potency *in Vitro*.** The inhibitory potency of β-peptides was measured using an *in vitro* assay (Table 1).[16] ELISA quantification of *de novo* generated Aβ40 and Aβ42 from recombinant substrates was performed in the presence of β-peptides. For comparison, the inhibitory activity of benchmark GSIs and their photoactivatable derivatives,[5,6,17−22] which are discussed in the Mode of Action section, was also examined (Table 2; see Supporting Information for chemical structures). The inhibitory activity became stronger with increasing β-peptide length; hexamers (**1** and **4**) showed no activity, whereas dodecamers (**3** and **6**) showed the strongest activity in this series of enantiomers. Interestingly, the β-peptides composed of (*S*,*S*)-ACPC were much more potent inhibitors than those composed of (*R*,*R*)-ACPC. A similar tendency was observed in the case of helical peptide inhibitors: D-peptides were more potent than their L-peptide counterparts.[5,23] In the case of β-peptides, the right-handed helices **4**−**6** were more effective than the left-handed helices **1**−**3** (β-peptides composed of (*R*,*R*)-ACPC were reported to form left-handed 12-helix[14]). This is the opposite tendency to what was seen with helical α-peptides: left-handed helical D-peptides were more potent than the right-handed L-peptides.[5,23] In the case of α-peptides, the advantage of D-peptides may arise from their resistance to proteolytic degradation. For the β-peptides, there is not an issue of proteolysis, so the observed preference might reflect the intrinsic substrate preference of the γ-secretase. Among the compounds tested, **6** showed the strongest inhibitory activity, being comparable to the benchmark GSIs.

***Table 2.*** Inhibitory Activity of Benchmark GSIs and Their Photoactivatable Derivatives Used in This Study in *in Vitro* Assay ($n = 3$)

| class | compounds | $IC_{50}$ for Aβ40 (nM) | $IC_{50}$ for Aβ42 (nM) |
|---|---|---|---|
| helical peptide | pep.11[a] | $6.67 \times 10^3$ | $6.83 \times 10^3$ |
| | pep.11-Bt | 37.9 | 12.8 |
| transition state analogue (TSA) | L-685,458 | $4.68 \times 10^{-1}$ | $5.48 \times 10^{-1}$ |
| | 31C | 40.2 | 32.1 |
| | 31C-Bpa | 44.6 | 37.5 |
| dipeptidic inhibitor | DAPT | $1.73 \times 10^2$ | $2.56 \times 10^2$ |
| | compound E (CE) | $7.54 \times 10^{-1}$ | $5.28 \times 10^{-1}$ |
| | DBZ (YO01027) | $5.82 \times 10^{-1}$ | $4.71 \times 10^{-1}$ |

[a] The difference in the potency of pep.11 compared with the previous report[5] may be due to the difference in the protocol of the *in vitro* assay system.

| Peptides | Sequence | Number of β-amino acids |
|---|---|---|
| 7 | Ac-$X^S X^S X^S X^S X^S X^S X^R X^S X^S X^S X^S X^S$-$NH_2$ | 12 |
| 8 | Ac-$X^S X^S X^S X^R X^S X^S X^S X^S X^R X^S X^S X^S$-$NH_2$ | 12 |

***Figure 3.*** Synthesized helicity-disrupted β-peptides.

**Helicity-Disrupted β-Peptides.** To test whether these peptides inhibit γ-secretase simply owing to their hydrophobicity or whether conformation is critical, we designed and synthesized helicity-disrupted β-peptides **7** and **8** by swapping one or two (*S*,*S*)-ACPC residue(s) for (*R*,*R*)-ACPC residue(s) (Figure 3). CD spectra of β-peptides **6**−**8** in methanol are presented in Figure 4. The decrease in intensity at 222 nm with additional

(14) Applequist, J.; Bode, K. A.; Appella, D. H.; Christianson, L. A.; Gellman, S. H. *J. Am. Chem. Soc.* **1998**, *120*, 4891–4892.
(15) Appella, D. H.; Christianson, L. A.; Klein, D. A.; Richards, M. R.; Powell, D. R.; Gellman, S. H. *J. Am. Chem. Soc.* **1999**, *121*, 7574–7581.
(16) Karlstrom, H.; Bergman, A.; Lendahl, U.; Naslund, J.; Lundkvist, J. *J. Biol. Chem.* **2002**, *277*, 6763–6766.
(17) Fuwa, H.; Takahashi, Y.; Konno, Y.; Watanabe, N.; Miyashita, H.; Sasaki, M.; Natsugari, H.; Kan, T.; Fukuyama, T.; Tomita, T.; Iwatsubo, T. *ACS Chem. Biol.* **2007**, *2*, 408–418.
(18) Morohashi, Y.; Kan, T.; Tominari, Y.; Fuwa, H.; Okamura, Y.; Watanabe, N.; Sato, C.; Natsugari, H.; Fukuyama, T.; Iwatsubo, T.; Tomita, T. *J. Biol. Chem.* **2006**, *281*, 14670–14676.
(19) Kan, T.; Tominari, Y.; Morohashi, Y.; Natsugari, H.; Tomita, T.; Iwatsubo, T.; Fukuyama, T. *Chem. Commun.* **2003**, 2244–2245.
(20) Esler, W. P.; Kimberly, W. T.; Ostaszewski, B. L.; Ye, W.; Diehl, T. S.; Selkoe, D. J.; Wolfe, M. S. *Proc. Natl. Acad. Sci. U.S.A.* **2002**, *99*, 2720–2725.
(21) Dovey, H. F.; et al. *J. Neurochem.* **2001**, *76*, 173–181.
(22) Li, Y. M.; Xu, M.; Lai, M. T.; Huang, Q.; Castro, J. L.; DiMuzio-Mower, J.; Harrison, T.; Lellis, C.; Nadin, A.; Neduvelil, J. G.; Register, R. B.; Sardana, M. K.; Shearman, M. S.; Smith, A. L.; Shi, X. P.; Yin, K. C.; Shafer, J. A.; Gardell. S. J. *Nature* **2000**, *405*, 689–694.
(23) Bihel, F.; Das, C.; Bowman, M. J.; Wolfe, M. S. *J. Med. Chem.* **2004**, *47*, 3931–3933.

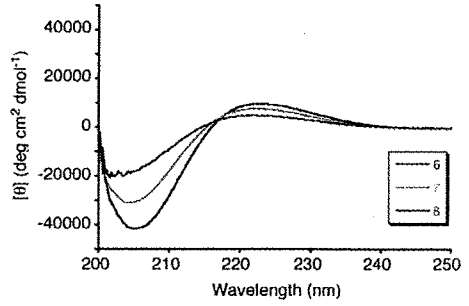


***Figure 4.*** CD spectra of β-peptides **6**–**8** in methanol. The molar ellipticity [θ] values have been normalized for oligomer concentration and the number of backbone amide groups.

***Table 3.*** Inhibitory Potency of β-Peptides **7**–**8** toward γ-Secretase

| compound | $IC_{50}$ (Aβ40, nM) | $IC_{50}$ (Aβ42, nM) |
|---|---|---|
| **7** | $6.89 \times 10^3$ | $>3.00 \times 10^4$ |
| **8** | $>3.00 \times 10^4$ | $>3.00 \times 10^4$ |

***Table 4.*** Inhibitory Potency of GSIs on HEK293/SC100gal4 Cells ($n = 3$)

| class | compounds | $IC_{50}$ for Aβ40 (nM) | $IC_{50}$ for Aβ42 (nM) | $IC_{50}$ for AICD (nM) |
|---|---|---|---|---|
| helical peptide | pep.11 | $>1.00 \times 10^4$ | $>1.00 \times 10^4$ | $7.84 \times 10^3$ |
| TSA | L-685,458 | $5.48 \times 10^3$ | $1.51 \times 10^4$ | $1.61 \times 10^3$ |
| dipeptidic inhibitor | DAPT | $2.45 \times 10^3$ | 57.4%[a] | $4.70 \times 10^2$ |
| β-peptide | **6** | 70.6 | 82.0 | 4.88 |

[a] Inhibition of 57.4% was observed at 30000 nM.

***Table 5.*** Inhibitory Potency of GSIs on N2a cells ($n = 3$)

| class | compounds | $IC_{50}$ for Aβ40 (nM) | $IC_{50}$ for Aβ42 (nM) |
|---|---|---|---|
| helical peptide | pep.11 | $>1.00 \times 10^4$ | $>1.00 \times 10^4$ |
| TSA | L-685,458 | $7.57 \times 10^2$ | $4.10 \times 10^3$ |
| dipeptidic inhibitor | DAPT | $8.63 \times 10^2$ | $1.93 \times 10^3$ |
| β-peptide | **6** | 95.6 | $2.21 \times 10^2$ |

(*R*,*R*)-ACPC replacements indicates that the population of the 12-helical state decreases as the number of (*R*,*R*)-ACPC residues increases. Replacement of a single monomer unit led to significant loss of inhibitory potency compared with the corresponding enantiomer (Table 3), suggesting that helical character is critical for the inhibitory potency of 12-helical β-peptides.

**Cell-Based Assay.** Next the inhibitory potency of β-peptides was measured using cell-based assay. ELISA quantifications of secreted Aβ40 and Aβ42 from HEK293/SC100gal4[24] (Table 4) or Neuro2a[25] cells (Table 5) in the presence of β-peptides were performed. The release of APP intracellular domain (AICD), a counterpart of Aβ, was also analyzed by Gal4-fused AICD-driven UAS-firefly luciferase activity in HEK293/SC100gal4 cells.[24] We found that **6** showed most potent inhibitory activity both in Aβ and AICD generation. Increase in the Aβ secretion ("Aβ rise") at low concentration of **6** was observed in a similar manner to that by benchmark GSIs,[26] presumably due to the aberrant trafficking and processing of the accumulated γ-secretase substrates (Figure 5). Finally, we confirmed that **6** inhibited the Aβ secretion accompanied with the accumulation of C-terminal stubs of endogenous APP in primary neuronal culture (Figure 6). These results suggest that the β-peptide directly targets the γ-secretase *in vivo*.

**Specificity of β-Peptide.** There is serious concern about adverse effects caused by GSIs that inhibit the release of Notch intracellular domain (NICD), a direct signaling molecule in the Notch pathway.[1–4] Thus, identification of a way to spare Notch-cleaving γ-secretase activity is considered mandatory for development of AD therapeutics. We examined the effect of β-peptides **5** and **6** on Notch cleavage in PS1-expressing #5/DKO cells (Table 6), which coexpress truncated APP and Notch with the corresponding luciferase reporter system (i.e., Gal4/VP16-fused AICD-driven UAS-firefly luciferase and NICD-driven TP1-*Renilla* luciferase, respectively). Intriguingly, both **5** and **6**, but not benchmark GSI DBZ, preferentially inhibited AICD over NICD generation, suggesting that the β-peptides show substrate specificity in a fashion similar to that of Notch-sparing GSI.[27] Then, we examined whether the β-peptides affect other proteases which target hydrophobic substrates, since the β-peptides are relatively hydrophobic. Treatment with **6** caused no significant change in the levels of sAPPα generated by α-secretase activity, suggesting that the β-peptide **6** had no effect on the membrane-bound metalloproteases ADAM9, -10, and -17 (Figure. 7).[28] Next, we tested the effect of β-peptide on the intramembrane cleaving protease, signal peptide peptidase (SPP). TSA-based GSI cross-inhibited the SPP activity, because PS and SPP share catalytic YD/GxGD motifs.[29] Moreover, we and others have reported that potent dipeptidic GSIs such as DBZ, but not DAPT, cross-inhibit SPP.[17,30,31] It is noteworthy that leucine-rich Aib containing helical peptides cross-inhibited the γ-secretase and SPP activities, but these compounds showed some preference for SPP activity.[32,33] These data suggest that the γ-secretase and SPP execute intramembrane cleavage with similar, but not identical, mechanisms. Unexpectedly, **6** had no effect on the SPP activity in cell-based assay, while **6** exhibited inhibitory activity against AICD generation comparable to that of DBZ (Table 6, Figure 8). Taken together, these data suggest that β-peptide **6** is one of the most potent peptide-based GSIs found thus far and represents a potential lead compound for the development of APP-cleaving γ-secretase activity-specific inhibitors.

**Mode of Action.** PS undergoes endoproteolysis to generate N-terminal and C-terminal fragments (NTF and CTF, respectively) in active γ-secretase complex.[1–4,34] Using pharmacologically distinct photoactivatable GSI derivatives, it is now widely accepted that (1) PS fragments represent the proteolytically active molecule, (2) PS fragments form an initial substrate docking site distinct from the catalytic site of the γ-secretase,

(24) Isoo, N.; Sato, C.; Miyashita, H.; Shinohara, M.; Takasugi, N.; Morohashi, Y.; Tsuji, S.; Tomita, T.; Iwatsubo, T. *J. Biol. Chem.* **2007**, *282*, 12388–12396.
(25) Tomita, T.; Maruyama, K.; Saido, T. C.; Kume, H.; Shinozaki, K.; Tokuhiro, S.; Capell, A.; Walter, J.; Grunberg, J.; Haass, C.; Iwatsubo, T.; Obata, K. *Proc. Natl. Acad. Sci. U.S.A.* **1997**, *94*, 2025–2030.
(26) Burton, C. R.; et al. *J. Biol. Chem.* **2008**, *283*, 22992–23003.
(27) Mayer, S. C.; et al. *J. Med. Chem.* **2008**, *51*, 7348–7351.
(28) Deuss, M.; Reiss, K.; Hartmann, D. *Curr. Alzheimer Res.* **2008**, *5*, 187–201.
(29) Fluhrer, R.; Haass, C. *Neurodegener Dis.* **2007**, *4*, 112–116.
(30) Nyborg, A. C.; Jansen, K.; Ladd, T. B.; Fauq, A.; Golde, T. E. *J. Biol. Chem.* **2004**, *279*, 43148–43156.
(31) Weihofen, A.; Lemberg, M. K.; Friedmann, E.; Rueeger, H.; Schmitz, A.; Paganetti, P.; Rovelli, G.; Martoglio, B. *J. Biol. Chem.* **2003**, *278*, 16528–16533.
(32) Sato, T.; Ananda, K.; Cheng, C. I.; Suh, E. J.; Narayanan, S.; Wolfe, M. S. *J. Biol. Chem.* **2008**, *283*, 33287–33295.
(33) Sato, T.; Nyborg, A. C.; Iwata, N.; Diehl, T. S.; Saido, T. C.; Golde, T. E.; Wolfe, M. S. *Biochemistry* **2006**, *45*, 8649–8656.
(34) Selkoe, D. J.; Wolfe, M. S. *Cell* **2007**, *131*, 215–221.

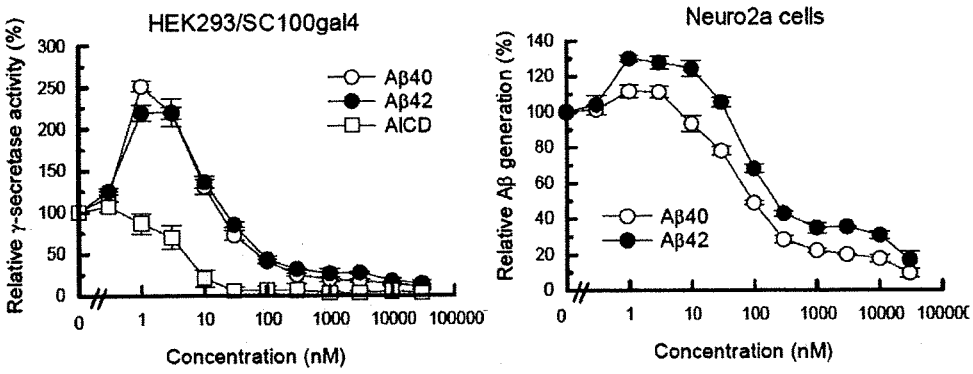


***Figure 5.*** Inhibitory effect of **6** on cell-based γ-secretase activity.

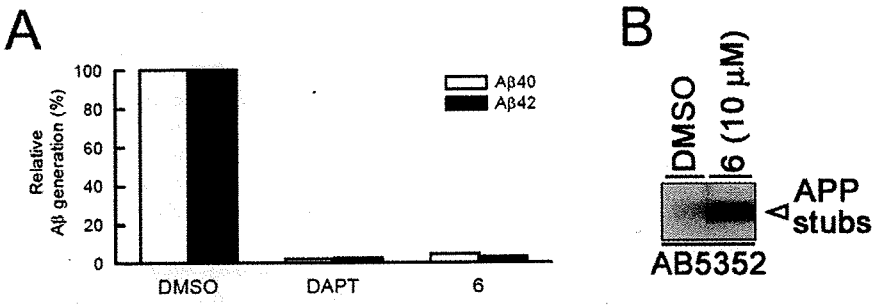


***Figure 6.*** Inhibitory effect of **6** on the γ-secretase activity in primary neuronal culture. (A) The levels of the secreted Aβ measured by ELISA. Concentration of DAPT or β-peptide **6** was 10 μM ($n = 4$, S.E.). (B) Detection of endogenous APP C-terminal stubs (*white arrowhead*) by immunoblotting with anti-APP antibody AB5352.

***Table 6.*** Inhibitory Potency of GSIs on PS1 Expressing #5/DKO cells ($n = 3$)

| class | compounds | $IC_{50}$ for AICD (nM) | $IC_{50}$ for NICD (nM) | notch selectivity |
|---|---|---|---|---|
| dipeptidic inhibitor | DBZ | 2.90 | 1.54 | 0.5 |
| β-peptide | **5** | 44.7 | $5.64 \times 10^2$ | 12.6 |
| | **6** | 3.70 | 18.9 | 5.1 |

(3) Substrates are transferred from the docking to the catalytic site through a transition path (see Figure 10A).[18] To elucidate the mode of action of the β-peptides, we examined the ability of these peptides to displace photoactivatable GSIs in a photoaffinity experiment. The labeling of PS1 NTF by Aib-containing helical pep.11-Bt, which directly targets the initial substrate docking site,[6] was completely abolished by preincubation with **5** or **6** (Figure 9A), suggesting that these β-peptides share the same binding site with pep.11. Unexpectedly, the biotinylation of PS1 by TSA-based photoprobe 31C-Bpa, that directly bound to the catalytic site,[35] was somewhat decreased by the β-peptides, while pep.11 increased the labeling of PS1

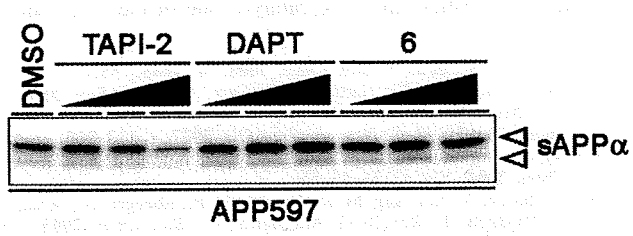


***Figure 7.*** Effect of **6** on the levels of the sAPPα secreted from Neuro2a cells. sAPPα (*white arrowheads*) was detected by immunoblotting using anti-APP ectodomain APP597. *Black triangles* on the lanes schematically represent concentrations of the inhibitors. TAPI-2 is a representative metalloprotease inhibitor.

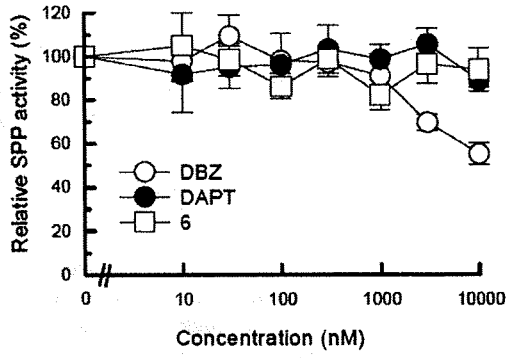


***Figure 8.*** Inhibitory effect of **6** on the SPP activity in cell-based assay.

(Figure 9B).[6] Next the effects of the β-peptides on the biotinylation by dipeptidic photoprobes (i.e., DAP-BpB and CE-BpB3) were examined.[17,18] Pep.11 decreased the biotinylation of PS1 by DAP-BpB, while the labeling by CE-BpB3 was increased as previously described.[17,36] In contrast, the β-peptides increased the labeling of PS1 by both DAP-BpB and CE-BpB3, suggesting that the β-peptides conferred an open conformation to the transit path. Taken together, these data support our notion that the β-peptides target the initial substrate docking site of the γ-secretase in a different fashion compared with pep.11.

A schematic depiction of γ-secretase cleavage is shown in Figure 10A.[17,18] Catalytic aspartates are shown as red circles

(35) Micchelli, C. A.; Esler, W. P.; Kimberly, W. T.; Jack, C.; Berezovska, O.; Kornilova, A.; Hyman, B. T.; Perrimon, N.; Wolfe, M. S. *FASEB J.* **2003**, *17*, 79–81.
(36) Takahashi, Y.; Hayashi, I.; Tominari, Y.; Rikimaru, K.; Morohashi, Y.; Kan, T.; Natsugari, H.; Fukuyama, T.; Tomita, T.; Iwatsubo, T. *J. Biol. Chem.* **2003**, *278*, 18664–18670.

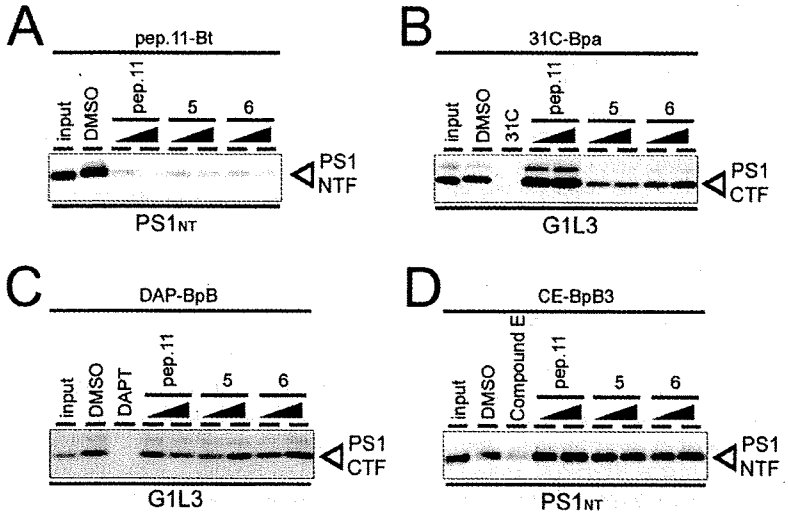


***Figure 9.*** Competition assay against photoaffinity labeling with pep.11-Bt (A), 31C-Bpa (B), DAP-BpB (C), and CE-BpB3 (D) in the presence of pep.11 or β-peptide **5** or **6**. The biotinylated PS1 fragments (*white arrowheads*) were detected by immunoblotting using antibodies against PS1 N terminus and loop region (PS1NT and G1L3, respectively). *Black triangles* on the lanes schematically represent concentrations of the competitors.

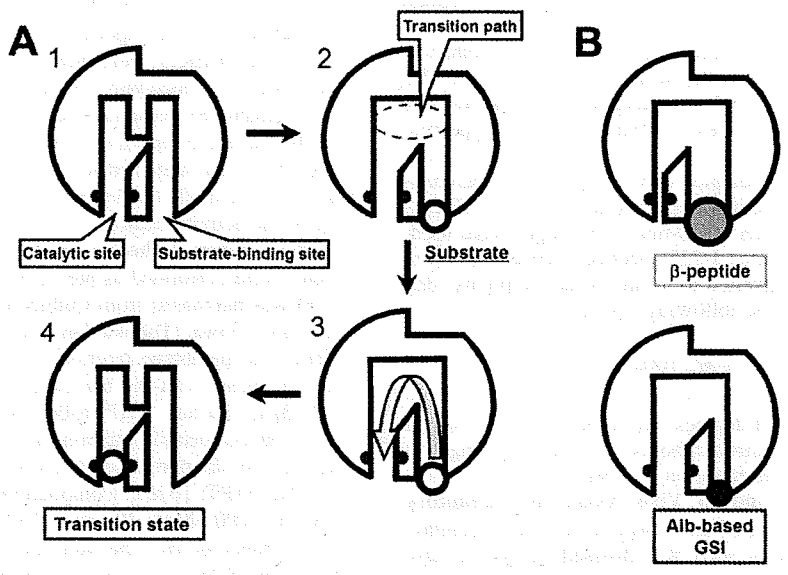


***Figure 10.*** Proposed mechanism of the γ-secretase cleavage and the effects of helical peptides. (A) Schematic depiction of the γ-secretase cleavage. (B) Putative inhibition modes of the β-peptide and Aib-based GSI.

at the catalytic site. Substrates enter the γ-secretase from the initial substrate docking site to the catalytic site through the transition path. In Figure 10B, putative inhibition modes of the β-peptide and Aib-based GSI are proposed. Both helical peptides target the initial substrate docking site. However, the occupation of the substrate binding site by the β-peptides allosterically narrows the catalytic site, while the binding of Aib-based GSI enlarges the conformational space of the catalytic site. These steric changes affected the labeling efficacy of PS1 by a photoprobe based on the transition-state analogue, 31C-Bpa, which directly targets the catalytic site.

## Conclusion

We have shown that a simple β-peptide foldamer acts as a highly potent GSI and that helical conformation is critical for this inhibition. β-Peptides composed of ACPC exhibit a strong tendency to adopt a specific helical conformation, 12-helix, and therefore may display side chains in predictable arrangements. Intriguingly, β-peptide presented here specifically inhibited the γ-secretase activity with substrate preference. Moreover, a chemical biological approach revealed that β-peptides directly target the initial substrate docking site of the γ-secretase. The present helical β-peptide inhibitor with activity at nanomolar concentration is expected to be a good lead compound for the development of γ-secretase-specific inhibitors and molecular tools to explore the substrate recognition of intramembrane proteases.

## Experimental Section

**Synthesis of β-Peptides.** Fmoc-*trans*-2-aminocyclopentanecarboxyic acid (Fmoc-ACPC-OH) was synthesized according to the reported procedure.[37] β-Peptides were synthesized with standard Fmoc solid phase methods. Fmoc-NH-SAL-PEG resin (0.24 mmol/g, 100–200 mesh, 1% DVB) was employed for all peptide synthesis. For a typical 20 μmol-scale synthesis: 83 mg of Fmoc-NH-SAL-PEG resin was swollen for 15 min in DMF. ***Coupling***

*cycles.* Three equivalents of Fmoc-ACPC-OH and 3 equiv of 2-(1*H*-benzotriazol-1-yl)-1,1,3,3-tetramethyluronium hexafluorophosphate (HBTU) and 3 equiv of 1-hydroxybenzotriazole monohydrate ($HOBt \cdot H_2O$) were dissolved in 300 $\mu$L of DMF, and 6 equiv of *N,N*-diisopropylethylamine (DIEA) was added. The solution was added to the resin bearing the N-deprotected $\beta$-peptide. The resin was agitated for 1−3 h. ***Fmoc deprotection cycles.*** Fmoc deprotection was accomplished by adding to the resin 1.0 mL of 20% (v/v) piperidine in DMF and rocking for 30 min. ***Acetylation.*** Acetylation of peptides was conducted for 2 h, by addition of 0.5 mL of 2:2:1 (v/v/v) $Ac_2O$/DMF/$Et_3N$ to the resin bearing the final desired N-deprotected $\beta$-peptide sequence. ***Cleavage.*** Cleavage of all $\beta$-peptides from resin was accomplished by shaking the resin in a solution of trifluoroacetic acid (TFA)/triisopropylsilane (TIPS)/$H_2O$ 95:2.5:2.5 (0.5 mL) for 2 h. The resin was removed *via* filtration and rinsed with additional TFA. The combined filtrate was concentrated under a stream of Ar. $\beta$-Peptides were precipitated from excess cold $Et_2O$, and isolated by centrifugation. The crude $\beta$-peptides thus obtained were purified by RP-HPLC using a linear gradient system from 30:70 to 70:30 isopropanol/$H_2O$ (0.1% TFA) over 40 min ($\beta$-peptides **1** and **4**), from 45:55 to 65:35 isopropanol/$H_2O$ (0.1% TFA) over 45 min ($\beta$-peptides **2** and **5**), from 50:50 to 65:35 isopropanol/$H_2O$ (0.1% TFA) over 45 min ($\beta$-peptides **3** and **6**), from 40:60 to 55:45 isopropanol/$H_2O$ (0.1% TFA) over 45 min ($\beta$-peptide **7**) at the flow rate of 2.1 mL/min. In the case of $\beta$-peptide **8**, the crude $\beta$-peptide was dissolved in formic acid and purified by RP-HPLC using a linear gradient of 70:30 to 95:5 methanol/$H_2O$ (0.1% TFA) over 45 min at the flow rate of 3.0 mL/min. The purities of $\beta$-peptides were ~95%, as measured by comparing peak areas in analytical HPLC traces at 220 nm (see Supporting Information).

**CD Spectra.** Dry peptide samples were weighed on a microanalytical balance and dissolved in an appropriate amount of HPLC-grade methanol. Sample cells of 10-mm path length were used. Data were collected on a Jasco J-725 spectropolarimeter at room temperature. Data were converted to mean residue ellipticity (deg $cm^2$ $dmol^{-1}$) according to the following equation:

$$[\Theta] = \psi M_r / 100lc$$

where $\psi$ is the CD signal in degrees, $M_r$ is the molecular weight divided by the number of chromophores, $l$ is the path length in decimeters, and $c$ is the concentration in g/mL.

**Protocol of in Vitro and in Vivo Assay for Inhibitory Activity.** Inhibitory potencies of the $\beta$-peptides on the $\gamma$-secretase activity were analyzed by *in vitro* or cell-based assays. *In vitro* $\gamma$-secretase assay was performed as described previously with some modifications.[36] *N*-[*N*-(3,5-Difluorophenacetyl)-L-alanyl]-(*S*)-phenylglycine *tert*-butyl ester (DAPT) was a gift from Dr. Fukuyama (The University of Tokyo).[19] L-685,458, pep.11, pep.11-Bt and TAPI-2 were purchased from Bachem, Ito Lifescience, BEX and BIOMOL, respectively. Purified recombinant substrate (C100-FLAG-myc-6xHis) was incubated together with solubilized HeLa cell membrane fraction (250 $\mu$g/mL) in $\gamma$ buffer (HEPES buffer containing 0.25% CHAPSO, 5 mM EDTA, 5 mM 1,10-phenanthroline, 10 mg/mL phosphoramidon, 0.01% phosphatidylcholine (Avanti) and Complete protease inhibitor mixture (Roche Applied Science)) at 37 °C. The samples were centrifuged, and the supernatants were analyzed by BNT77/BA27 or BNT77/BC05 ELISAs for *de novo* generation of A$\beta$. For cell-based assays, HEK293 cells stably overexpressing SC100gal4, EGFP and UAS-firefly luciferase (HEK293/SC100gal4) or Neuro2a cells were cultured in the presence of various concentrations of the compounds for 24 h. Primary neuronal culture from mouse embryo was obtained as previously described.[38] Neurons were cultured with GSIs at DIV 6 and incubated for 24 h. Cultured media were collected and subjected to BNT77/BA27 or BNT77/BC05 ELISAs to measure the levels of secreted A$\beta$. The levels of APP C-terminal stubs were analyzed by immunoblotting using anti-APP antibody AB5352 (Millipore). To analyze the effect on the sAPP$\alpha$ generation, Neuro2a cells were treated with TAPI-2 (0.2, 2, 20 $\mu$M), DAPT (0.1, 1, 10 $\mu$M) or **6** (0.1, 1, 10 $\mu$M) for 24 h, and conditioned medium was subjected to immunoblotting against sAPP$\alpha$ (APP597, IBL, Japan). For generation of #5/DKO cells, retroviral expression vectors containing SPC99gvp-6myc (modified SPA4CT[39] fused with Gal4/VP16 and hexa-myc epitope tag) in pMXs-puro,[40,41] NΔE-6myc (truncated mouse Notch[42] fused with hexa-myc epitope tag) in pLPCX (Clontech), UAS-firefly luciferase in pMXs-EGFPII and TP1-*Renilla* luciferase in pMXs-II were constructed. pMXs-EGFPII is a derivative encoding EGFP instead of puromycin resistance gene in pMXs-puroII.[43] pMXs-II was generated by an excision of puromycin resistance gene in pMXs-puroII. All plasmids were transfected into retrovirus packaging cell line, Plat-E.[41] Recombinant retroviruses were inoculated with immortalized fibroblasts obtained from *Psen1*$^{-/-}$; *Psen2*$^{-/-}$ knockout mouse (DKO cells).[44] Infected DKO cells were further selected with puromycin to obtain #5/DKO cells as previously described.[40,41] Before GSI treatment, recombinant retrovirus encoding PS1 was infected into #5/DKO cells. The GSI-treated cell lysates were subjected to the luciferase assay to measure the AICD- and NICD-generating activity.[24]

**SPP Assay.** SPP reporter assay was performed as previously described.[30] HEK293 cells were transiently transfected with expression plasmids encoding *Renilla* luciferase, human SPP[45] and recombinant SPP substrate fused with ATF6[30] together with ERSE-firefly luciferase reporter vector.[46] The cell lysate was harvested after 24 h and subjected to the luciferase assay to measure SPP activity. The firefly luciferase activity was normalized to the *Renilla* luciferase activity control.

**Photoaffinity Labeling Study.** Photoaffinity labeling experiments were performed as previously described.[17,18] Compound E (CE) was purchased from Calbiochem or kindly provided by Dr. Haruhiko Fuwa (Tohoku University). 1% CHAPSO-solubilized HeLa cell membrane fractions were diluted to 0.25% CHAPSO and incubated with the photoaffinity probes (pep11-Bt; 100 nM, 31C-Bpa; 100 nM, DAP-BpB; 100 nM, CE-BpB3; 30 nM) at 4 °C. In the competition experiments, the solubilized membranes were mixed with the parent compounds (pep.11; 2.5 and 25 $\mu$M, 31C; 10 $\mu$M, DAPT; 10 $\mu$M, Compound E; 3 $\mu$M) or the $\beta$-peptides (**5**; 300 and 3000 nM, **6**; 30 and 300 nM), prior to the addition of the photoaffinity probe. The samples were irradiated on ice using a UV lamp. SDS was added to the labeled samples to give a final concentration of 1% w/v, and the solution was incubated with Dynabeads M-280 (Invitrogen). Biotinylated proteins were eluted from the resin by boiling for 1 min in Laemmli sample buffer. The labeled proteins were detected by immunoblotting using anti-

(37) LePlae, P. R.; Umezawa, N.; Lee, H.-S.; Gellman, S. H. *J. Org. Chem.* **2001**, *66*, 5629–5632.

(38) Fukumoto, H.; Tomita, T.; Matsunaga, H.; Ishibashi, Y.; Saido, T. C.; Iwatsubo, T. *Neuroreport* **1999**, *10*, 2965–2969.

(39) Lichtenthaler, S. F.; Multhaup, G.; Masters, C. L.; Beyreuther, K. *FEBS Lett.* **1999**, *453*, 288–292.

(40) Watanabe, N.; Tomita, T.; Sato, C.; Kitamura, T.; Morohashi, Y.; Iwatsubo, T. *J. Biol. Chem.* **2005**, *280*, 41967–41975.

(41) Kitamura, T.; Koshino, Y.; Shibata, F.; Oki, T.; Nakajima, H.; Nosaka, T.; Kumagai, H. *Exp. Hematol.* **2003**, *31*, 1007–1014.

(42) Kopan, R.; Schroeter, E. H.; Weintraub, H.; Nye, J. S. *Proc. Natl. Acad. Sci. U.S.A.* **1996**, *93*, 1683–1688.

(43) Kamura, T.; Hara, T.; Matsumoto, M.; Ishida, N.; Okumura, F.; Hatakeyama, S.; Yoshida, M.; Nakayama, K.; Nakayama, K. I. *Nat. Cell Biol.* **2004**, *6*, 1229–1235.

(44) Herreman, A.; Serneels, L.; Annaert, W.; Collen, D.; Schoonjans, L.; De Strooper, B. *Nat. Cell Biol.* **2000**, *2*, 461–462.

(45) Grigorenko, A. P.; Moliaka, Y. K.; Soto, M. C.; Mello, C. C.; Rogaev, E. I. *Proc. Natl. Acad. Sci. U.S.A.* **2004**, *101*, 14955–14960.

(46) Yoshida, H.; Haze, K.; Yanagi, H.; Yura, T.; Mori, K. *J. Biol. Chem.* **1998**, *273*, 33741–33749.

$PS1_{NT}$[47] (kindly provided by Dr. Gopal Thinakaran, The University of Chicago) or anti-G1L3 antibody.[48]

**Acknowledgment.** We thank Drs. G. Thinakaran (The University of Chicago), B. De Strooper (KU Leuven), U. Strobl (Helmholtz Zentrum München), A. Nyborg, T. Golde (Mayo Clinic), A. P. Grigorenko, E. I. Rogaev (University of Massachusetts), H. Fuwa, M. Sasaki (Tohoku University), T. Kitamura, S. Yokoshima, T. Fukuyama (The University of Tokyo), K. Mori (Kyoto University), K. I. Nakayama (Kyushu University), R. Kopan (Washington University in St. Louis), Takeda Pharmaceutical Company and lab members for valuable reagents, helpful discussions and technical assistance. We also thank Prof. H. Sajiki and Dr. Y. Monguchi (Gifu Pharmaceutical University) for HRMS-FAB analysis. This work was supported in part by Grants-in-Aid for Scientific Research (A) (T.H.), Young Scientists (S) from Japan Society for the Promotion of Science (JSPS) (T.T), by the Targeted Proteins Research Program of the Japan Science and Technology Corporation (JST) (T.I., T.T.), and Uehara Memorial Foundation (N.U.). N.W. was a research fellow of JSPS.

**Supporting Information Available:** Chemical structures of benchmark GSIs and their photoactivatable derivatives, identification of β-peptides **1**−**8**, synthesis of 31C-Bpa; complete refs 21, 26, and 27. This material is available free of charge via the Internet at http://pubs.acs.org.

JA9001458

(47) Thinakaran, G.; Harris, C. L.; Ratovitski, T.; Davenport, F.; Slunt, H. H.; Price, D. L.; Borchelt, D. R.; Sisodia, S. S. *J. Biol. Chem.* **1997**, *272*, 28415–28422.

(48) Tomita, T.; Takikawa, R.; Koyama, A.; Morohashi, Y.; Takasugi, N.; Saido, T. C.; Maruyama, K.; Iwatsubo, T. *J. Neurosci.* **1999**, *19*, 10627–10634.

THE JOURNAL OF BIOLOGICAL CHEMISTRY VOL. 284, NO. 41, pp. 27838–27847, October 9, 2009


# Single Chain Variable Fragment against Nicastrin Inhibits the γ-Secretase Activity*[S]

Received for publication, August 11, 2009 Published, JBC Papers in Press, August 14, 2009, DOI 10.1074/jbc.M109.055061

**Ikuo Hayashi[‡1], Sho Takatori[‡1], Yasuomi Urano[§], Hiroko Iwanari[§¶], Noriko Isoo[‡], Satoko Osawa[‡], Maiko A. Fukuda[‡], Tatsuhiko Kodama[§], Takao Hamakubo[§], Tong Li[‖], Philip C. Wong[‖], Taisuke Tomita[‡**2], and Takeshi Iwatsubo[‡**‡‡]**

*From the [‡]Department of Neuropathology and Neuroscience, Graduate School of Pharmaceutical Sciences, The University of Tokyo, 7-3-1 Hongo, Bunkyo-ku, Tokyo 113-0033, Japan, the [§]Laboratory for Systems Biology and Medicine, Research Center for Advanced Science and Technology, The University of Tokyo, 4-6-1 Komaba, Meguro-ku, Tokyo 153-8904, Japan, [¶]Perseus Proteomics, Inc., 4-7-6 Komaba, Meguro-ku, Tokyo 153-0041, Japan, the [‖]Department of Pathology, The Johns Hopkins University School of Medicine, Baltimore, Maryland 21205, and **Core Research for Evolutional Science and Technology, Japan Science and Technology Corporation, and the [‡‡]Department of Neuropathology, Graduate School of Medicine, The University of Tokyo, 7-3-1 Hongo, Bunkyo-ku, Tokyo 113-0033, Japan*

**γ-Secretase is a membrane protein complex that catalyzes intramembrane proteolysis of a variety of substrates including the amyloid β precursor protein of Alzheimer disease. Nicastrin (NCT), a single-pass membrane glycoprotein that harbors a large extracellular domain, is an essential component of the γ-secretase complex. Here we report that overexpression of a single chain variable fragment (scFv) against NCT as an intrabody suppressed the γ-secretase activity. Biochemical analyses revealed that the scFv disrupted the proper folding and the appropriate glycosyl maturation of the endogenous NCT, which are required for the stability of the γ-secretase complex and the intrinsic proteolytic activity, respectively, implicating the dual role of NCT in the γ-secretase complex. Our results also highlight the importance of the calnexin cycle in the functional maturation of the γ-secretase complex. The engineered intrabodies may serve as rationally designed, molecular targeting tools for the discovery of novel actions of the membrane proteins.**

γ-Secretase catalyzes intramembrane proteolysis of a variety of substrates including amyloid β precursor protein (APP)[3] to generate amyloid β peptide (Aβ), the latter being a major component of senile plaques in the brains of Alzheimer disease patients. Thus, agents that inhibit γ-secretase activity could serve as an effective therapeutics for Alzheimer disease, whereas the γ-secretase activity plays important roles in cell signaling pathways including Notch signaling (1, 2). γ-Secretase consists of at least four integral membrane proteins, *i.e.* presenilin (PS), nicastrin (NCT), APH-1, and PEN-2, all of which are essential to the proteolytic activity (3–5). Molecular cellular and chemical biological analyses have revealed that PS forms a hydrophilic pore involving the transmembrane domain 6 and 7, where conserved catalytic aspartates reside to function as catalytic residues of γ-secretase complex (6, 7). APH-1 is a multipass membrane protein that plays a role in stabilization and trafficking of the γ-secretase complex (8), and PEN-2 is a cofactor for the activation and the regulation of the γ-secretase activity (3, 9).

NCT, which was identified as a PS-binding protein (10), is a single-pass membrane protein that harbors an extracellular domain (ECD) with a number of *N*-glycosylation sites. In mammalian cells NCT undergoes Endo H-resistant complex glycosylation and acquires trypsin resistance during the assembly process of the γ-secretase complex (11–17). Molecular and cellular analyses revealed that the trypsin resistance, presumably indicating the proper structural folding of NCT, might be directly linked to the enzymatic activity, whereas the complex glycosylation is dispensable. Moreover, multiple sequence alignment analyses revealed that NCT ECD have a similarity to an aminopeptidase (18), whereas certain catalytic residues are not conserved. Recently one study has suggested that NCT plays a critical role in substrate recognition (19). During the proteolytic process, NCT ECD captures the most N terminus of the substrate as a primary substrate receptor (*i.e.* exosite) for the γ-secretase via the aminopeptidase-like domain. However, this view has been recently challenged (20). Nevertheless, as structural information of NCT ECD is totally lacking, the functional role of the structural maturation of NCT in the formation and activity of the γ-secretase remains unclear.

Molecular engineering of monoclonal antibodies opens a venue for the functional analyses of targeted molecule and the therapeutic intervention for several diseases (21). A single-

* This work was supported in part by grants-in-aid for Young Scientists (S) from the Japan Society for the Promotion of Science, Scientific Research on Priority Areas Research on Pathomechanisms of Brain Disorders from the Ministry of Education, Culture, Sports, Science, and Technology, Japan, by the Program for Promotion of Fundamental Studies in Health Sciences of the National Institute of Biomedical Innovation, by Targeted Proteins Research Program of the Japan Science and Technology Corporation (JST), and by Core Research for Evolutional Science and Technology of JST, Japan.

[S] The on-line version of this article (available at http://www.jbc.org) contains supplemental Figs. 1–3.

[1] Research Fellows of the Japan Society for the Promotion of Science.

[2] To whom correspondence should be addressed: Dept. of Neuropathology and Neuroscience, Graduate School of Pharmaceutical Sciences, The University of Tokyo, 7-3-1 Hongo, Bunkyo-ku, Tokyo 113-0033, Japan. Tel.: 81-3-5841-4868; Fax: 81-3-5841-4708; E-mail: taisuke@mol.f.u-tokyo.ac.jp.

[3] The abbreviations used are: APP, amyloid-β precursor protein; Aβ, amyloid-β peptide; CHAPSO, 3-[(3-cholamidopropyl)dimethylammonio]-2-hydroxy-1-propanesulfonate; CNX, calnexin; CST, castanospermine; CTF, C-terminal fragment; NCT, nicastrin; PS, presenilin; Endo H, endoglycosidase H; ECD, extracellular domain; ER, endoplasmic reticulum; scFv, single chain variable fragment.

chain antibody fragment (scFv) is comprised of heavy- and light-chain sequences of an antibody linked by a short linker and preserves binding abilities of its parental antibody. scFv can be expressed intracellularly as an intrabody (22, 23), which provides a powerful method for phenotypic knock-out of the genes. Intrabodies have been investigated as treatments for a variety of pathological conditions, including neurodegenerative diseases such as Parkinson disease and Huntington disease. Moreover, several recent publications have highlighted the therapeutic potential of intrabodies targeting intra- as well as extracellular epitopes (24–29). Here, we generated scFv against NCT from an anti-NCT monoclonal antibody. Unexpectedly, the overexpression of the anti-NCT scFv as an intrabody abolished the proteolytic activity by the destabilization of the γ-secretase complex and the inappropriate glycosylation of NCT. This is the first example showing that engineered antibody would be a useful tool for the direct modulation of the γ-secretase complex and its activity.

## EXPERIMENTAL PROCEDURES

*Plasmids*—C-terminal V5-His-tagged human NCT ECD inserted in pBlueBac4.5 (Invitrogen) was generated from NCT/V5-His in pBlueBac4.5 (30) by long PCR. Cytoplasmic RNA was prepared from $1 \times 10^7$ hybridoma cells by using Isogen reagent (Nippongene, Tokyo, Japan). The cells were lysed by mixing with Isogen and incubated at room temperature for 5 min. After centrifugation of the lysate, the RNA was precipitated and dissolved in distilled water. This RNA was used as a template for first-strand cDNA synthesis with 3′ primers specific for the mouse IgG genes (Novagen, Darmstadt, Germany). The cDNA fragments were then amplified by PCR with LA Taq (Takara, Shiga, Japan) using 3′ and 5′ primers from the mouse Ig primer set as per the manufacturer's instructions (Ig-Prime kit protocols; Novagen). The PCR products were subcloned into the pEF6/V5-His-TOPO vector (Invitrogen) by the TOPO cloning method. scFv cDNAs inserted into pSecTag2C (Invitrogen) were constructed as follows. The PCR-derived DNA fragments in pEF6/V5-His TOPO were subjected to splice overlapping extension PCR to connect heavy- and light-chain genes to give a single fusion protein gene. In the first round PCR, heavy- and light-chain genes were amplified by using the following primers: the variable region heavy-chain gene, 5′-ggggaattcGAAGTGAAGCTGGTGGAG-3′ (VHF#1) and 5′-caccacctccggaaccaccaccaccggaaccaccacctccGGCTGAGGAGACTGTGAGAGT-3′ (VHR#1); the variable region light-chain genes, 5′-ggtggttccggtggtggtggttccggaggtggtggttcaGACATTGTGCTGACACAGTCT-3′ (VLF#1) and 5′-cccgcggccgcTTTTATTTCCAGCTTGGT-3′ (VLR#1) or 5′-ggtggttccggtggtggtggttccggaggtggtggttcaGATATCCAGATGACACAGACT-3′ (VLF#2) and 5′-cccgcggccgcTTTGATTTCCAGCTTGGT-3′ (VLR#2). In the second round PCR, the amplified heavy- and light-chain fragments were linked by using VHF#1 and VLR#1 or #2. The amplified scFv cDNAs were digested with EcoRI and NotI to subclone into the EcoRI-NotI-digested pSecTag2C vector. Wild-type as well as mutant (*i.e.* Δ312, 648ATAA) human NCT inserted in the pEF6/V5-His-TOPO was generated as previously described (14). All cDNAs were sequenced by automated sequencer (LI-COR, Lincoln, NE). cDNAs encoding deletion mutants of human NCT fused with V5 tag were kindly gifted from Drs. Keiro Shirotani and Christian Haass (Ludwig-Maximilians-University, Munich, Germany) (17).

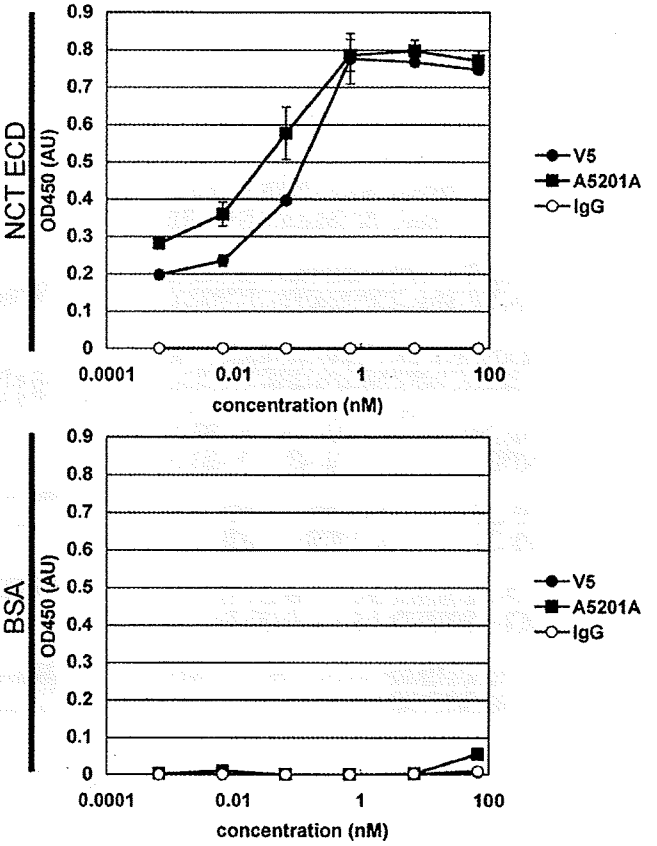


FIGURE 1. **Binding of A5201A to recombinant NCT ECD.** Sequentially diluted A5201A, anti-V5 monoclonal antibody, or mouse IgG fraction was applied to NCT ECD- or bovine serum albumin-coated plates. Subsequently, anti-mouse IgG antibody conjugated with horseradish peroxidase was incubated, and monoclonal antibody binding was quantitated by measuring $A_{450}$ using peroxidase substrate. *AU*, absorbance units.

*Cell Culture and Transfection*—Maintenance of Sf9 cells, transfection, and recombinant baculovirus preparation were done as previously described (30, 31). Hybridoma cells were maintained in RPMI 1640 medium supplemented with L-glutamine (Nikken Bio Medical Laboratory, Kyoto, Japan) containing 15% (v/v) fetal bovine serum, 100 international units/ml of penicillin, 100 μg/ml of streptomycin, and 1 mM sodium pyruvate (Sigma) at 37 °C in 5% $CO_2$. All transfections were achieved by FuGENE 6 (Roche Applied Science) according to the manufacturer's instructions. HEK293 cell lines stably expressing scFv were selected by Zeocin (Invitrogen). *Ncstn* knock-out fibroblasts (NKO cells) (32) stably expressing wild-type and mutant NCT were selected by Blasticidin (Calbiochem).

*Purification of NCT ECD and Secreted scFv*—For NCT ECD production, Sf9 cells were infected with recombinant virus encoding NCT ECD at multiplicity of infection 2 and incubated for 72 h. For scFv, 5201F-expressing cells (clone 2) were incubated in regular media for 72 h. NCT ECD or scFv was recovered from the culture media by using a nickel-chelating column (GE Healthcare). Bound proteins were eluted by a stepwise gradient of imidazole (5–300 mM) in phosphate-buffered saline.

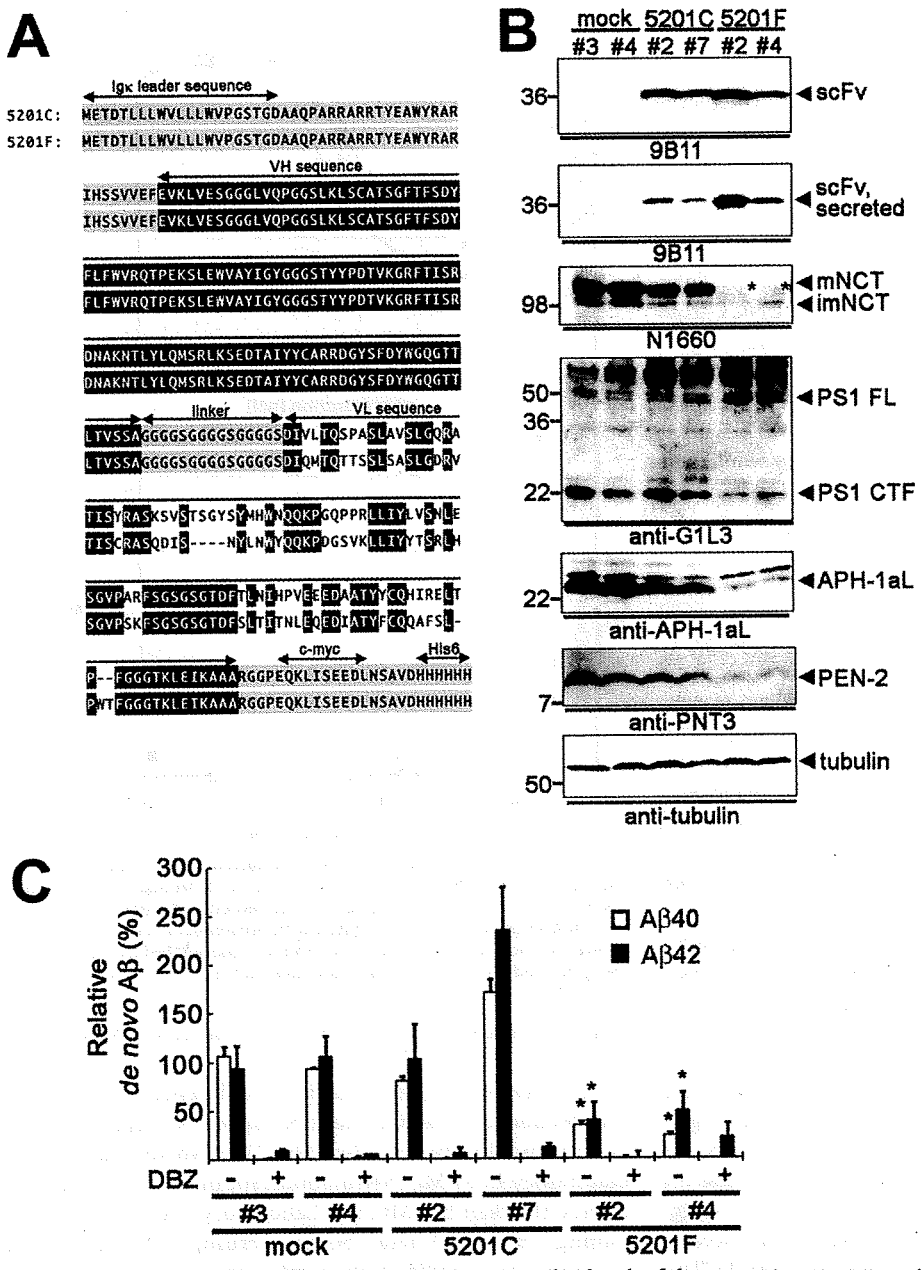


FIGURE 2. **Effects of overexpression of 5201F on the expression levels of the γ-secretase components and proteolytic activity.** *A*, the sequence alignment of the obtained scFvs, 5201C, and 5201F. *B*, immunoblot analysis of HEK293 cells stably expressing intrabodies with each antibody, indicated *below the panel*. *mNCT* and *imNCT* represent mature and immature NCT, respectively. *FL*, full-length. Mature NCT with faster migration in 5201F-expressing cells (NCT*) was indicated by an *asterisk*. *C*, specific γ-secretase activity of the intrabody-expressing cells measured by *in vitro* assay. Solubilized cell membranes were coincubated with the substrates in the presence (+) or absence (−) of 100 nM DBZ. *De novo* generation levels of Aβ40 (*open columns*) or Aβ42 (*filled columns*) peptides were normalized by the γ-secretase levels, which were assessed by densitometric analysis of PS1 CTF on the immunoblotting ($n = 3$, *, $p < 0.01$, Student's *t* test).

Eluted fractions were analyzed by Coomassie or silver staining as well as immunoblotting.

*Analysis of A5201A Binding Ability by Enzyme-linked Immunosorbent Assay*—Purified NCT ECD or bovine serum albumin was coated on 96-well plates at the concentration of 2 μg/ml in a coating buffer (0.1 M sodium bicarbonate, pH 8.6), and the plates were incubated overnight at 4 °C. After the coating, the plates were blocked by a blocking buffer (phosphate-buffered saline containing 1× BlockAce (Dainippon Sumitomo Pharma, Osaka, Japan) and 0.02% (w/v) sodium azide) and stored at 4 °C until used. A5201A, anti-V5 antibody (Invitrogen), as a positive control or mouse IgG fraction (SIGMA) as a negative control was added at various concentrations to the wells, and the plates were incubated overnight at 4 °C. Binding of antibody was detected by anti-mouse IgG antibody conjugated with horseradish peroxidase (GE Healthcare) and tobacco mosaic virus substrate. $A_{450}$ was measured and quantitated by SpectraMax M2 microplate reader (Molecular Devices, Sunnyvale, CA).

*Antibodies, Immunological Analyses, and in Vitro γ-Secretase Assay*—Anti-G1Nr3, G1L3, and PNT3 polyclonal antibodies against glutathione *S*-transferase-fused human PS1 N terminus, cytoplasmic loop region, or synthetic peptide corresponding to the N-terminal 26 amino acids of human/mouse PEN-2, respectively, were previously described (30, 33–35). Anti-PS1NT polyclonal antibody was kindly gifted from Drs. Gopal Thinakaran and Sangram Sisodia (The University of Chicago, Chicago, IL). Other antibodies were purchased from Cell Signaling Technology (Danvers, MA) (anti-c-*myc* (9B11)), Covance (Princeton, NJ) (anti-APH-1aL (O2C2)), Santa Cruz Biotechnology (Santa Cruz, CA) (anti-NCT N terminus (N19)), Sigma (anti-NCT C terminus (N1660), anti-α-tubulin (DM1A)), or Stressgen (Ann Arbor, MI) (anti-Calnexin). Cells were solubilized with HEPES buffer (10 mM HEPES, pH 7.4, 150 mM NaCl) containing 1% (w/v) CHAPSO. Immunoprecipitation, immunoblot analysis, metabolic labeling, and enzymatic digestion experiments were previously described (14, 33–36). For detection of the γ-secretase activity *in vitro*, solubilized HeLa cell membranes were co-incubated with the APP-based recombinant substrates in the presence (+) or absence (−) of 100 nM DBZ (YO01027), which was kindly provided from Dr. Haruhiko Fuwa (Tohoku University, Miyagi, Japan) (3, 37–39). Aβ was quantified by human β

amyloid enzyme-linked immunosorbent assay kit (WAKO, Osaka, Japan). Cell surface biotinylation was performed using Pierce cell surface protein isolation kit (Pierce) according to the manufacturer's instruction.

## RESULTS

*Anti-NCT Intrabody Decreases the Expression Levels of NCT and Suppresses the γ-Secretase Activity*—Budded baculovirus from Sf9 cells infected with recombinant virus displays the recombinant proteins on its virion membrane (30, 40). Thus, budded baculovirus can be used as an optimal immunogen to generate monoclonal antibodies against the membrane proteins. Using this technology, we have generated a monoclonal antibody A5201A that specifically binds to NCT ECD. A5201A showed specific binding ability to V5-tagged NCT ECD in a similar manner to anti-V5 antibody, whereas an irrelevant IgG exhibited no reactivity (Fig. 1). Next, we generated two intrabodies based on A5201A, named 5201C and 5201F. Both intrabodies consist of light and heavy chain variable regions that were cloned from hybridoma cells producing A5201A, conjugated with three GGGGS pentapeptide repeats as a linker by PCR. Each cDNA was cloned into a pSecTag2C vector, which enables the targeting of the intrabodies into the lumen by the Igκ leader sequence and detection with *c-myc* tag attached to the C terminus (Fig. 2*A*). 5201C and 5201F harbored a difference only in the light chain variable region sequences, whereas the heavy chain variable region sequences were totally identical. As NS-1 cells, the mouse myeloma cells used for the generation of the hybridoma (40) endogenously express κ light chain gene, one of the two light chain sequences might be derived from NS-1 cells.

We then generated HEK293 cell lines stably expressing 5201C or 5201F (Fig. 2*B*, supplemental Fig. S1). Immunoblot analysis revealed that both intrabodies were expressed intracellularly as a ~36-kDa protein and secreted into culture media. Intriguingly, the expression levels of NCT, especially that of mature NCT, were markedly reduced in 5201F-expressing cell lines, and the remaining "mature-like" NCT showed slightly longer migration on SDS-PAGE than that of mock- or 5201C-expressing cells. Hereafter, we refer to this mature-like NCT of ~115 kDa observed in 5201F-expressing cells as NCT*. Moreover, the protein levels of other components of the γ-secretase complex, *i.e.* PS1, APH-1aL, and PEN-2, were also decreased in 5201F-expressing cells. In contrast, none of the γ-secretase components was affected in 5201C-expressing cells. Next, we examined whether the intrinsic γ-secretase activity was affected in the intrabody-expressing cells by *in vitro* assay using an APP-based recombinant substrate (3, 38). We then normalized the activity against the levels of PS1 CTF to measure the specific activity per active complex (20). 5201F-expressing cells showed significant reduction in the Aβ-generating activities (for Aβ40, 34.5% (#2) and 23.9% (#4) compared with that of mock cells; for Aβ42, 21.3% (#2) and 39.4% (#4)) (Fig. 2*C*). These results suggest that the overexpression of intrabody 5201F, but not 5201C, reduces the steady-state expression levels as well as the intrinsic activity of the γ-secretase complex.

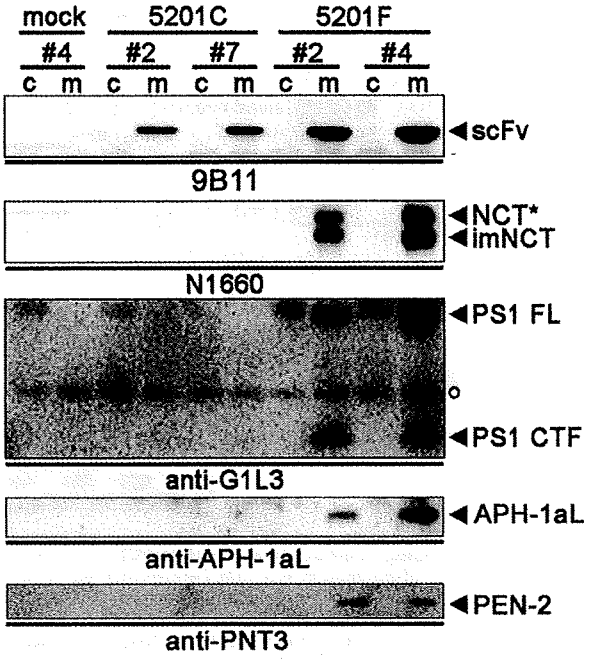


FIGURE 3. **Incorporation of 5201F into the γ-secretase complex.** Co-immunoprecipitation analysis of 1% CHAPSO-solubilized fractions from intrabody-expressing stable HEK293 cells with control IgG (*c*) or anti-*c-myc* antibody 9B11 (*m*). Immunoprecipitates were analyzed by immunoblotting with each antibody indicated *below the panel*. The *white circle* indicates the immunoglobulin chain. *imNCT* immature NCT.

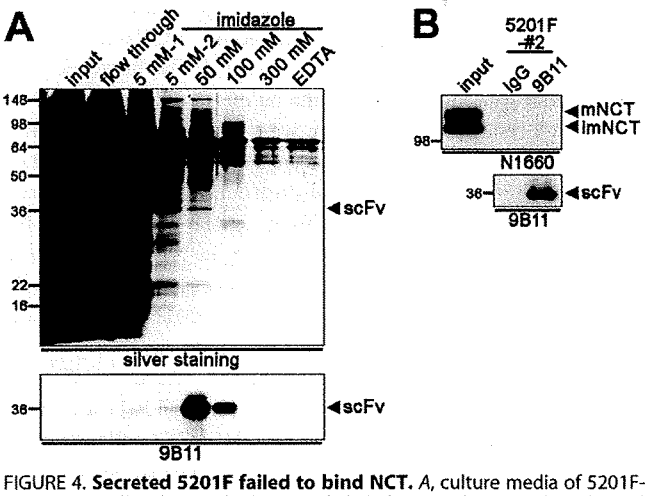


FIGURE 4. **Secreted 5201F failed to bind NCT.** *A*, culture media of 5201F-expressing cells were applied to a nickel chelating column, and the bound proteins were eluted with stepwise increased concentrations of imidazole and EDTA. Eluates were dialyzed against phosphate-buffered saline and then analyzed with silver staining (*upper panel*) and immunoblotting with anti-*c-myc* antibody 9B11 antibody (*lower panel*). *B*, partially purified secreted scFv from the 100 mM imidazole fraction in *A* was mixed with 1% CHAPSO-solubilized HEK293 cell lysates and immunoprecipitated with control IgG or anti-*c-myc* 9B11 antibody. Immunoprecipitates were analyzed by immunoblotting using each antibody indicated *below the panels*. Note that secreted scFv failed to bind with endogenous NCT. *mNCT* and *imNCT* represent mature and immature NCT, respectively.

*5201F, but Not 5201C, Binds to NCT ECD in the γ-Secretase Assembly Process*—We then examined the interactions of the intrabodies with the γ-secretase complex by immunoprecipitation analysis. NCT* as well as immature NCT were co-precipitated with intrabody only from 5201F-expressing cells (Fig. 3).

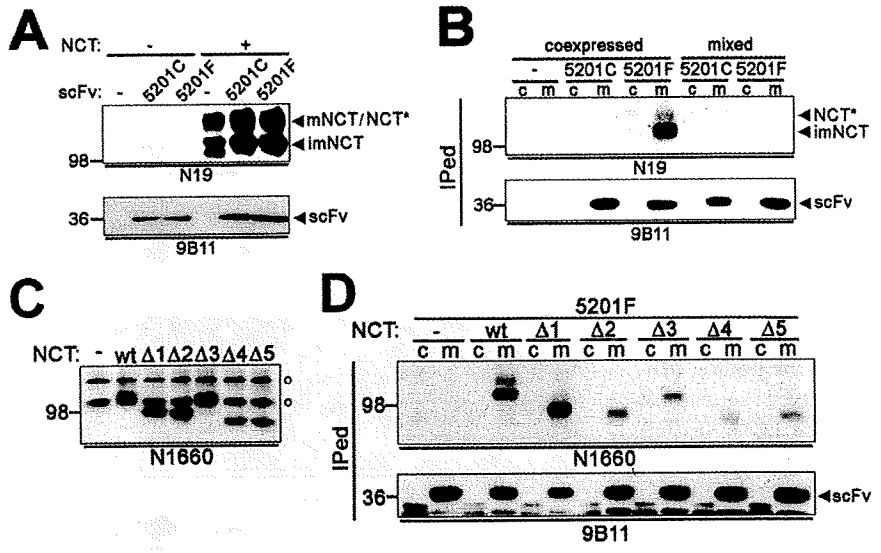


FIGURE 5. **Direct binding of intracellular 5201F to NCT.** *A*, immunoblotting of the NKO cells overexpressing intrabodies with or without human NCT. *mNCT* and *imNCT* represent mature and immature NCT, respectively. *B*, immunoprecipitation (*IPed*) of 1% CHAPSO-solubilized NKO cells with control IgG (*c*) or anti-c-*myc* antibody 9B11 (*m*). *Coexpressed* samples were the lysates from NKO cells coexpressing intrabodies and human NCT. *Mixed* samples were the mixture of the lysate from NKO cells either expressing intrabodies or NCT. *C*, immunoblotting of the NKO cells coexpressing the deletion mutant of human NCT together with 5201F. *White circles* indicate nonspecific proteins appeared in NKO cells. *D*, immunoprecipitation of 1% CHAPSO-solubilized NKO cells in *C* with anti-c-*myc* antibody 9B11.

All γ-secretase components were also detected in the immunoprecipitates with 5201F. These data suggest that 5201F directly interacts with NCT and that 5201F-bound NCT is incorporated into the γ-secretase complex. Unexpectedly, however, 5201F purified from conditioned media failed to pull down NCT from HEK cell lysates (Fig. 4). Then, we transiently expressed intrabody in the presence or absence of human NCT in NKO cells (32) and performed the immunoprecipitation analysis using mixed lysates. The coexpressed 5201F precipitated NCT polypeptides, whereas the intrabody in NKO cells failed to interact with the independently expressed NCT (Fig. 5, *A* and *B*), suggesting that the intrabody 5201F is incorporated into the γ-secretase complex during its assembly process. Moreover, significant reduction of mature NCT was observed in stable NKO cells coexpressing 5201F and human NCT in a similar manner to that in HEK293 cells expressing 5201F, suggesting that 5201F was able to form NCT* in NKO cells (supplementary Fig. S2). Next, we analyzed the location of the epitope of the intrabody 5201F using systematically deleted constructs (NCT/Δ1-Δ5) of NCT ECD (17) in NKO cells. Previous results have suggested that these deletion constructs encode loss-of-function mutant forms of NCT. Although 5201F bound to all deletion NCT mutants, the immunoreactivities against NCT/Δ2, Δ3, Δ4, and Δ5 were significantly reduced, suggesting that 5201F directly recognizes a broad region in NCT ECD irrespective of the formation of functional γ-secretase complex (Fig. 5, *C* and *D*). Collectively, these results suggest that the intracellularly expressed scFv 5201F directly targets the nascent or newly synthesized NCT polypeptides during the biosynthetic pathway and is incorporated into the γ-secretase complex.

*Binding of 5201F Prevents the Glycosyl and the Structural Maturation of NCT*—During the maturation process of the γ-secretase complex, NCT ECD undergoes a complex glycosylation and a conformational change to acquire trypsin resistance along with the trafficking from ER to the cell surface (11–17). To investigate the molecular mechanism by which the binding of 5201F decreased the expression levels of NCT as well as of the γ-secretase components, we biochemically characterized NCT*. In the metabolic labeling experiment, NCT was synthesized as ~110-kDa core-glycosylated intermediate form of polypeptides at 0 h of chase (Fig. 6*A*) (11, 13). The levels of NCT core polypeptides were comparable among the stable cell lines, indicating that the overexpression of intrabodies had no effect on the translation efficiency of NCT. Three hours after synthesis, measurable levels of NCT were converted to the 100 kDa immature form by trimming of glucose and mannose in the ER. Then these NCT matured into the complex glycosylated forms that exhibited retarded migration at 120 kDa. This mature NCT was long-lived, and significant levels of labeled mature NCT were still present 48 h after labeling as previously reported (11). In 5201F-expressing cells, however, the levels of immature NCT were relatively low at 3 h of chase and the conversion to NCT* was completed within 6 h. Moreover, 48 h after synthesis, NCT* was still present but clearly lesser in amount compared with that of mature NCT in mock- or 5201C-expressing cells, suggesting that the binding of 5201F caused rapid and inappropriate maturation of NCT polypeptides and rendered the NCT* unstable.

Next we examined the glycosylation state of NCT* by Endo H digestion. Mature NCT in mock- or 5201C-expressing cells was Endo H-resistant and migrated at ~120 kDa in SDS-PAGE, whereas immature NCT was completely deglycosylated as previously described (Fig. 6*B*) (11–17). Unexpectedly, NCT* showed Endo H resistance, too. Moreover, cell surface biotinylation experiments revealed that mature NCT* was displayed on the plasma membrane in a similar manner to the mature NCT of the control cell lines (Fig. 6*C*). The levels of PS1 N-terminal fragment in mock- and 5201F-expressing cells were almost comparable (supplemental Fig. S3), suggesting that the steady-state level of the γ-secretase complex containing 5201F on the cell surface is not significantly altered. Finally, we examined the trypsin resistance of NCT*. As previously described (17), substantial levels of mature NCT in mock- or 5201C-expressing cells remained intact after 30-min of incubation with trypsin, whereas immature NCT was completely digested (Fig. 6*D*). In contrast, in 5201F-expressing cells, NCT* was completely digested by trypsin in a similar manner to that

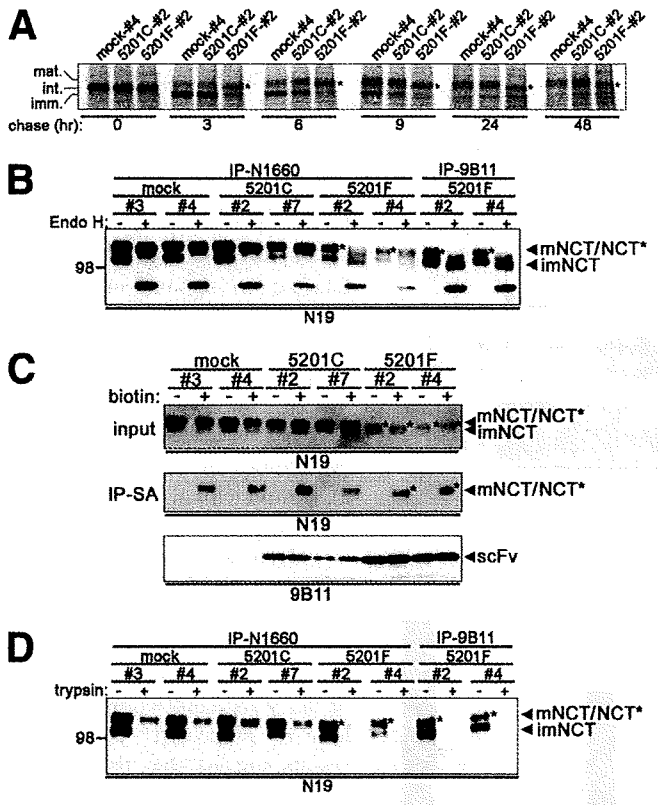


FIGURE 6. **Characterization of NCT* observed in 5201F-expressing cells.** *A*, metabolic labeling of stable HEK293 cells. Cells were pulse-labeled with [$^{35}$S]methionine and cysteine for 30 min and chased for indicated time periods. Lysates were immunoprecipitated with anti-NCT C terminus antibody N1660 and analyzed. NCT* is denoted by *asterisks*. *mat.*, mature; *imm.*, immature; *int.*, intermediate. *B*, immunoblotting of NCT polypeptides digested by Endo H. Immunoprecipitates (*IP*) with anti-NCT C terminus antibody N1660 or anti-c-*myc* antibody 9B11 were incubated with (+) or without (−) Endo H and analyzed by immunoblotting with anti-NCT N terminus antibody N19. *C*, cell surface biotinylation of HEK293 cells. Cell lysates (*input*) as well as biotinylated proteins (*IP-SA*) were analyzed using each antibody indicated *below the panels*. *D*, trypsin digestion of NCT polypeptides. Immunoprecipitates with anti-NCT C terminus antibody N1660 or anti-c-*myc* antibody 9B11 were incubated with (+) or without (−) 100 μg/ml trypsin and analyzed as in *B*.

of immature NCT. These results indicate that the binding of 5201F partially prevents the conformational as well as glycosyl maturation of NCT.

*Conformational Maturation of NCT Is Required for the Stabilization of the γ-Secretase Complex*—Large deletions in NCT ECD caused total loss of function of NCT (*i.e.* NCT/Δ1-Δ5) by failure in acquiring conformational maturation (10, 17). However, it is difficult to analyze the effect of the conformational defects in NCT ECD using these mutants because of the nature of deletion mutation; in fact, the overexpression of NCT/Δ312 in NKO cells completely failed to generate mature NCT (Refs. 10, 14, and 17; see below). To test whether a "partial" conformational defect of NCT affects the intrinsic γ-secretase activity, we introduced amino acid substitutions into the highly conserved residues at the juxtamembrane region of NCT ECD (*i.e.* Trp-648, Glu-650, and Ser-651 to alanine; 648ATAA), which play an important functional role in the γ-secretase complex formation (Fig. 7*A*) (41). The overexpression of NCT/648ATAA in NKO cells partially rescued the generation of mature NCT and PS1 fragments (Fig. 7*B*). Cycloheximide treatment caused rapid degradation of PS1 CTF in NCT/648ATAA-overexpressing cells, whereas PS1 CTF in cells expressing wild-type NCT was stable as previously reported (42), indicating that the reconstituted γ-secretase complex by NCT/648ATAA mutant is unstable (Fig. 7*C*). The trypsin digestion experiment revealed that mature NCT/648ATAA was readily degraded, suggesting that mutant NCT failed to acquire the conformational maturation, thereby causing the instability of the γ-secretase complex (Fig. 7*D*). The *de novo* Aβ generating activity in NCT/648ATAA-expressing NKO cells was also decreased (66.3% of that in wild-type human NCT-expressing cells). Notably, however, the *de novo* activity normalized by PS1 CTF levels in cells expressing NCT/648ATAA was not reduced compared with that in wild-type human NCT-expressing cells (Fig. 7*E*). These data suggest that the defect in the conformational maturation of NCT ECD caused the decrease in the total Aβ generating activity by loss of stability of the functional γ-secretase complexes, whereas the intrinsic activity of the enzyme was unaltered.

*Glucose Trimming in ER Is Required for the Intrinsic Activity of the γ-Secretase Complex*—*N*-Glycosylated proteins are folded by ER-resident chaperones (e.g., calnexin (CNX) or calreticulin) that recognize a monoglucose on unfolded polypeptides (43, 44). During the folding process, the transfer and the trimming of glucose are executed by the ER-resident glucosyltransferase and glucosidase, respectively. Thus, unfolded, but still glucose-attached proteins are captured by CNX to be folded; this process is called "the CNX cycle." To test the possibility that the CNX cycle is involved in the maturation of NCT, the immunoprecipitation analysis was performed. We confirmed the association of CNX and NCT as previously described (Fig. 8*A*) (45). Moreover, this interaction was significantly reduced by the overexpression of 5201F (Fig. 8*B*), suggesting that the glucose trimming and/or the CNX cycle would be inhibited by the scFv. Castanospermine (CST) is an α1,2-glucosidase inhibitor that causes the inhibition of interaction between *N*-linked glycoproteins and CNX (46, 47). The CST treatment caused the accumulation of aberrant NCT polypeptides, which presumably represent the glucosylated form of NCT (glucoNCT) (Fig. 9*A*). Intriguingly, glucoNCT showed a similar molecular weight to that of NCT* and acquired the Endo H resistance (Fig. 9*B*). In contrast, the levels of the γ-secretase components and the trypsin resistance of NCT were unaffected, suggesting that the glucose trimming is dispensable for the proper folding of NCT and the trafficking of the stable γ-secretase complex (Fig. 9, *A* and *C*). However, specific *de novo* Aβ generating activity normalized by PS1 CTF levels in CST-treated cell membrane was significantly decreased to a similar extent to that in 5201F-expressing cells (for Aβ40, 32.0% compared with that of mock-treated cells; for Aβ42, 33.4%) (Fig. 9*D*). These data indicate that the proper glucose trimming of NCT ECD accompanied by the CNX cycle is required for the intrinsic γ-secretase activity but not for the formation of the stable enzyme complex. Taken together, the binding of scFv 5201F has detrimental effects both on the

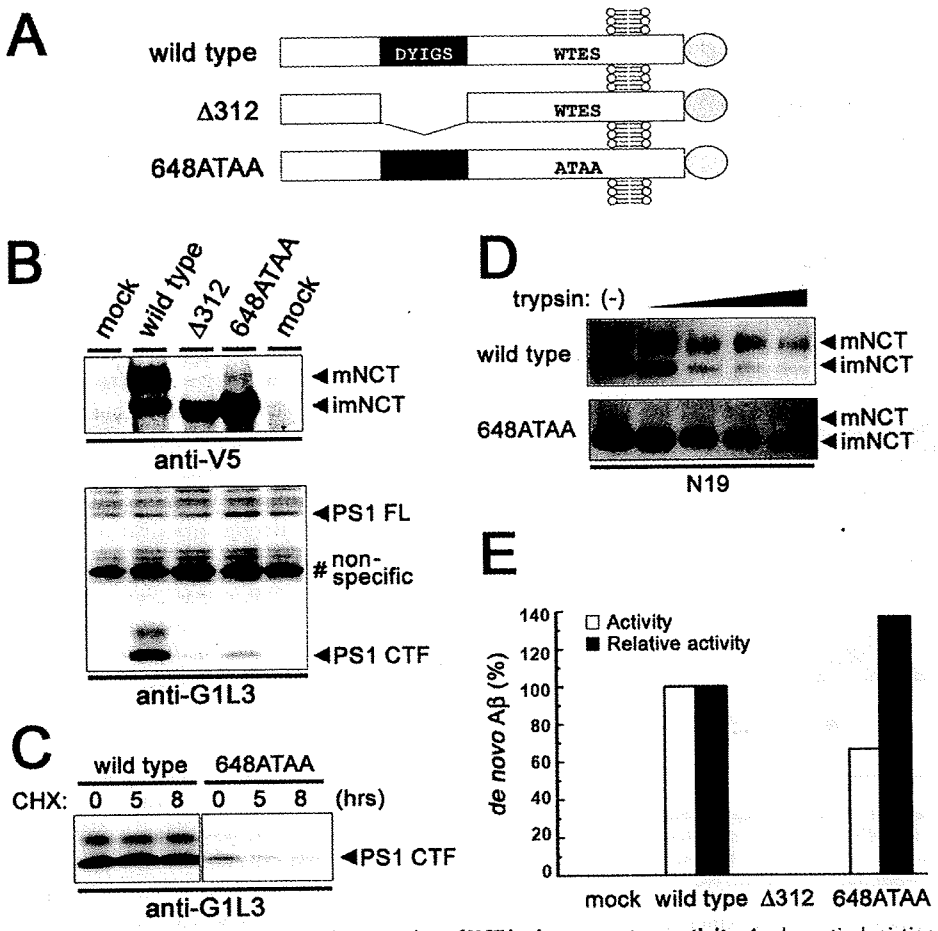


FIGURE 7. **The role of conformational maturation of NCT in the γ-secretase activity.** *A*, schematic depiction of NCT mutants analyzed in this experiment. The *black box* indicates highly conserved region containing DYIGS motif (312–369). The C-terminal V5 tag is indicated by *shaded circle*. *B*, immunoblot analysis of wild-type and mutant NCT-expressing NKO cell lysates. *mNCT* and *imNCT* represent mature and immature NCT, respectively. *C*, immunoblot analysis of wild-type and mutant NCT expressing NKO cells treated with cycloheximide (*CHX*) as previously reported. Lysates were prepared after cycloheximide treatment for various incubation times as indicated *above the lanes*. *D*, trypsin digestion of wild-type or mutant NCT polypeptides. *E*, *de novo* γ-secretase activity of the mutant NCT-expressing cells measured by *in vitro* assay. *White bars* indicate the proteolytic activity in the solubilized membrane containing equal protein amounts. *Black bars* denote the relative activity normalized by the γ-secretase levels, which were assessed by densitometric analysis of PS1 CTF on immunoblotting.

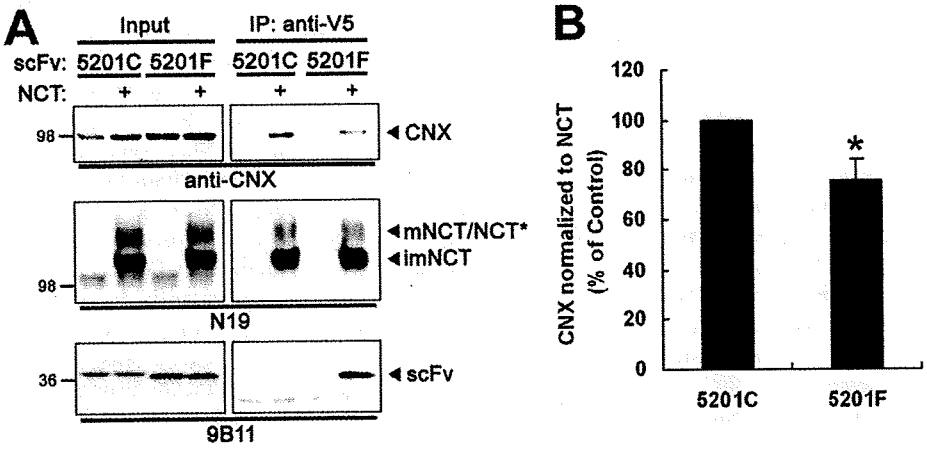


FIGURE 8. **Interaction of CNX and NCT.** *A*, immunoprecipitation (*IP*) analysis of NKO cell lysate transiently coexpressing human NCT and intrabodies. Immunoreactivities of NCT-bound CNX were quantified and normalized by the amount of total NCT in *B* ($n = 7$; *, $p < 0.05$, Student's *t* test).

conformational maturation and the glucose trimming of NCT ECD, thereby causing the destabilization and the loss of the enzymatic activity of the γ-secretase complex, respectively.

## DISCUSSION

Recently, much attention is being focused on the use of scFv fragments as intrabodies. Intrabodies have been used for phenotypic knock-out of endogenous target proteins by several different strategies. In this study we generated two intrabodies by using an anti-NCT ECD monoclonal antibody A5201A as a template. Biochemical analyses revealed that the specific binding of 5201F on NCT ECD inhibited the conformational change and the proper glycosylation of NCT, thereby causing the destabilization of the γ-secretase complex and the loss of proteolytic activity. Our results suggest that the functional maturation of NCT ECD regulates the proper trafficking, stability, and the specific activity of the γ-secretase complex.

γ-Secretase is an unusually stable protease that has >24 h of half-life in mammalian cells (42). Biochemical studies have shown that NCT forms a subcomplex with APH-1 within the biosynthetic pathway (48) and functions as a stabilizing cofactor as well as a substrate receptor for the γ-secretase complex (19, 20). The assembly of the γ-secretase complex occurs in the ER (49, 50), and only "functionally" assembled γ-secretase is subsequently sorted out to the Golgi apparatus in Rer1- and COPII-regulated manners (5, 51–53). However, the molecular information on the quality control of a prefunctional γ-secretase complex in the ER remains unknown. Here, we showed that the overexpression of 5201F caused an inappropriate glycosylation and prevented NCT polypeptides from acquiring the trypsin resistance, thereby causing the phenotypic "knock-out" of the γ-secretase components. Notably, we found that 5201F accelerated the inappropriate

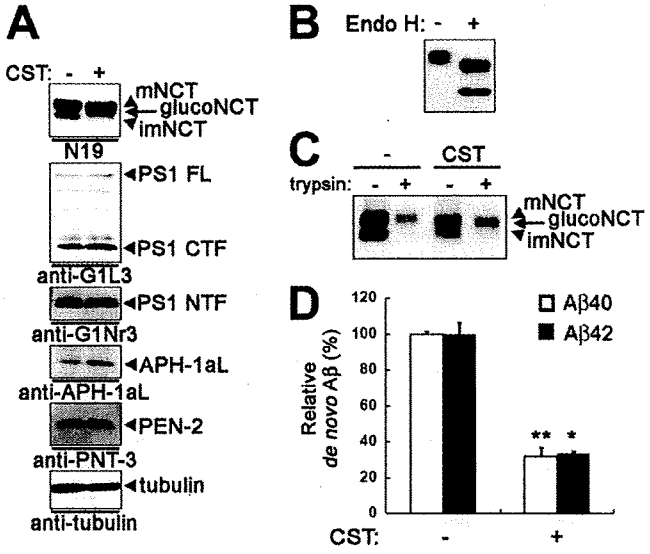


FIGURE 9. **The role of glucose trimming in NCT maturation and the γ-secretase activity.** *A*, immunoblot analysis of CST-treated HEK293 cell lysates. Note that CST treatment caused the accumulation of aberrant molecular weight NCT (*glucoNCT*). *mNCT* and *imNCT* represent mature and immature NCT, respectively. *NTF*, N-terminal fragment. *B*, Endo H and *C*, trypsin digestion of glucoNCT accumulated by CST treatment. *D*, specific γ-secretase activity of the CST-treated HEK293 cells analyzed by *in vitro* assay as in Fig. 1*C* ($n = 3$; *, $p < 0.01$, Student's *t* test).

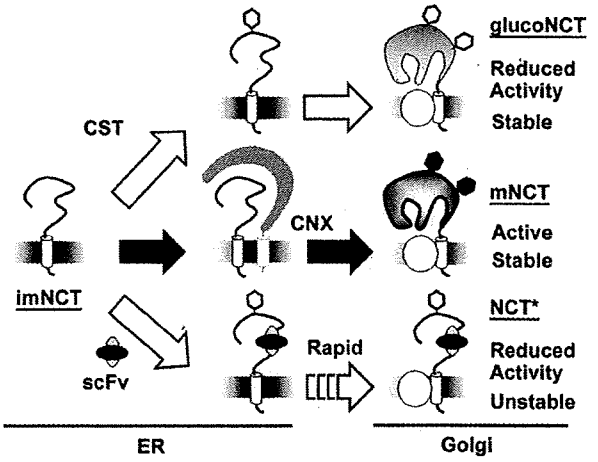


FIGURE 10. **A putative model for the mode of action of 5201F.** In biosynthetic pathway of the γ-secretase (*black arrows*), folding and glycosylation states of NCT are monitored by CNX in the ER. After the assembly of the γ-secretase complex together with PS, APH-1, and PEN-2 (*white circle*), NCT ECD is glycosylated with complex oligosaccharides (*black hexagon*) in the Golgi. CST treatment yields the stable γ-secretase complex containing NCT with aberrant glycosylation (*white hexagon*), which reduces the proteolytic activity. 5201F binding to NCT ECD inhibits the functional folding and glucose trimming to form the unstable and inactive γ-secretase complex with NCT*. *mNCT* and *imNCT* represent mature and immature NCT, respectively.

Endo H-resistant glycosylation of NCT, suggesting that the quality control and the trafficking system for the prefunctional γ-secretase in the ER are altered upon 5201F expression. In general, the folding and maturation states of glycoproteins are monitored by the CNX cycle. Properly folded glycoproteins escape this cycle and are sorted out from the ER. Trypsin resistance of NCT is tightly correlated with the proteolytic activity of the γ-secretase complex and may reflect its structural change in the ER (17), whereas the molecular basis of this conformational change has not been clarified to date. Of note, NCT fused with ER retention dilysine signal at the C terminus retained the ability to form the functional γ-secretase complex and is sorted out to the cell surface (49, 50). In addition, after trypsin digestion, the immunoreactivity of the C terminus of mature NCT was preserved, and no molecular weight change was observed (17). These results suggest that the most C terminus of NCT is also tightly folded in the functional γ-secretase complex. Thus, the folding state of NCT throughout the molecule might be under surveillance by ER-associated chaperones (*i.e.* CNX) and/or trafficking-related molecules (*e.g.* Rer1, coatmer subunits) as a molecular signature for the functional assembly of the γ-secretase complex. Incorporation of 5201F would interrupt the functional folding of NCT and the binding with CNX; the latter presumably caused the aberrant escape of the γ-secretase complex from the CNX cycle, thereby leading to the destabilization of the γ-secretase complex.

An ineffective CNX cycle is also caused by the inhibition of glucose trimming. The treatment with CST induced the accumulation of the glucosylated NCT polypeptides and reduced the γ-secretase activity. In general, aberrant glucosylated proteins generated by CST treatment are rapidly transported out from the ER or degraded by ER-associated degradation (46, 54, 55). However, our results showed that biochemical characteristics of the γ-secretase were unaffected by CST, whereas the intrinsic proteolytic activity was reduced. In contrast, it has been shown that treatment by kifunensine, which inhibits the mannose trimming occurring at the later stage of glycosyl maturation, has no effect on the γ-secretase activity (16, 17), suggesting that the glucose/mannose trimming was dispensable for the proper folding of NCT and the formation of the γ-secretase complex. Rather, our data indicate that the glucosyl state of NCT *per se* is involved in the specific enzymatic activity, suggesting the functional significance of the CNX cycle in the biogenesis of the γ-secretase complex. The analysis of 648/ATAA mutant NCT also supported our notion that the conformational maturation of NCT determines the amount, but not the intrinsic activity, of the functional γ-secretase complex. Although the molecular mechanism(s) by which the glycosylation of NCT modulates the intramembrane cleavage remain unknown, aberrant glucosylated NCT might have lesser activity in the substrate-capturing function.

We propose a model for the mode of action of 5201F as depicted in Fig. 10. NCT would be an essential component in the γ-secretase complex with dual functions, which were disrupted by the binding with 5201F. The properly glycosylated and folded NCT might function not only as a substrate receptor (19) but as a gatekeeper for the trafficking and the stability of the γ-secretase complex (20). Our data presented here also expand the repertoire of antibody-based functional reagents valuable for the cell biology research on the γ-secretase. To modify/engineer their binding profile, scFvs can be applicable to phage display, to which "rational design and directed molecular evolution" process with high throughput platform is applicable (56). In addition, structural studies using scFv have provided crucial information for the rational development of the small compound targeting protein-protein interactions (57).